An investigation of initialisation strategies for dynamic temperature optimisation in beer fermentation

An investigation of initialisation strategies for dynamic temperature optimisation in beer fermentation

Alistair D. Rodman, Dimitrios I. Gerogiorgis*

School of Engineering, University of Edinburgh, The King's Buildings, Edinburgh, EH9 3FB, UK

*****Corresponding author: D.Gerogiorgis@ed.ac.uk (+44 131 651 7072)

ABSTRACT

A wide range of optimisation methodologies exist for solving optimal control trajectory problems. With most approaches it is necessary to solve iteratively, starting from an initialising solution (often referred to as an initial guess). In this paper we investigate the performance of two different dynamic optimisation strategies for batch beer fermentation temperature control, using different initialisation profiles. A sequential method, Control Vector Parametrisation (CVP) is demonstrated as unable to produce solution profiles satisfying the industrially imposed undesirable by-product species concentration constraints. An alternative simultaneous method, Complete Parameterisation (CP), is employed in order to determine solutions satisfying these essential industrial production constraints. Blind initialisation guesses (isothermal profiles) have been shown to produce solution profiles not suitable for implementation on real fermentors; more promising candidate profile initialisations yield superior solutions. The use of a state-of-art NLP solver (IPOPT) with analytical first derivatives achieves remarkable solution robustness, eliminating initialisation and discretisation level dependence.

1. Introduction

1.1 Dynamic Optimisation Background

The problem of achieving optimal batch reactor operation via systematic optimisation methods has received considerable attention in the previous decades to serve the production of biochemical and polymer products, prompting novel deterministic (Wajge and Gupta, 1994; Arpornwichanop et al., 2005; Zavala et al., 2005) and stochastic (Ferrari et al., 2010; Zapata et al., 2010; Patel and Padhiyar, 2017) optimisation approaches, as well as other computational methods, e.g. the robust Design of Experiments (DoE) methodology (Mohan et al., 2005).

A wide range of dynamic optimisation methodologies exist for solving optimal control trajectory problems. These include variational methods and finite approximation methods. In the former exploiting Pontryagin's maximum principle allows the resulting two point boundary value problem to be solved, while the later uses predefined functional forms to represent the control profile (Almeida and Secchi, 2011). Finite formulations may be tackled with simultaneous, sequential or multi shooting strategies which are extensively reviewed in the literature (Biegler et al., 2002). The sequential strategy, control vector parameterisation (CVP), involves discretisation of the control profile with the ODE system (process model), requiring regular re-integration during the algorithm to compute corresponding state trajectories, an approach effective for problems with few decision variables and constraints (Osorio et al., 2005) which has been widely applied to engineering problems (e.g. Farhat et al., 1990; Mujtaba and Macchietto, 1993; Sørensen et al., 1996). In contrast, simultaneous strategies require the ODE system to also be discretised on the time horizon to produce a large scale NLP problem requiring no further integration of the DEA system, generally using orthogonal collocation techniques. The later, often referred to as complete parameterisation (CP), can offer numerous benefits, potentially being faster to solve problems with a greater number of decision variables and constraints (Cervantes et al., 1998; 2000).

With any approach it is necessary to solve iteratively, meaning that an initialising solution (often referred to as an initial guess) is necessary. Where robust globally optimal algorithms able to obtain solutions from any initialising profile (initial guess independent) cannot be applied certain problems can show sensitivity to the initialisation strategy employed. In this paper we investigate the performance of two different dynamic optimisation strategies for batch beer fermentation temperature control, using different initialisation solution profiles to elucidate the robustness of either strategy for batch fermentation optimisation.

1.2 Process Description

1.2.1 Beer Fermentation Background

Fermentation is an essential step in the manufacture of alcoholic beverages, responsible for the characteristic taste of the final product and of course its alcohol content. Upstream processing produces a sugar rich intermediate (wort) from a feedstock starch source (most typically malted barley). Once cooled to an appropriate initial temperature the wort enters stainless steel vessels along with yeast, allowing fermentation to commence. The primary chemical reaction pathway is the conversion of sugars into ethanol and carbon dioxide, which is coupled with biomass (yeast) growth and heat generation from the exothermic reaction. Concurrently, a range of species are formed at low concentrations by a multitude of side reactions, many of which may impact product flavour above threshold concentrations. Fermentation is completed once all consumable sugars have been converted by the yeast into alcohol, following which the solution leaves the fermenter for subsequent downstream processing prior to sale and consumption.

1.2.2 Fermentation modelling

Numerous models for the beer fermentation process have been published (Gee and Ramirez, 1988; de Andres-Toro, 1998, Trelea et al., 2001). The reduced-order models consider only the key species present as to system complexity (Vanderhaegen et al., 2006) leads to exhaustive modelling becoming unviable.

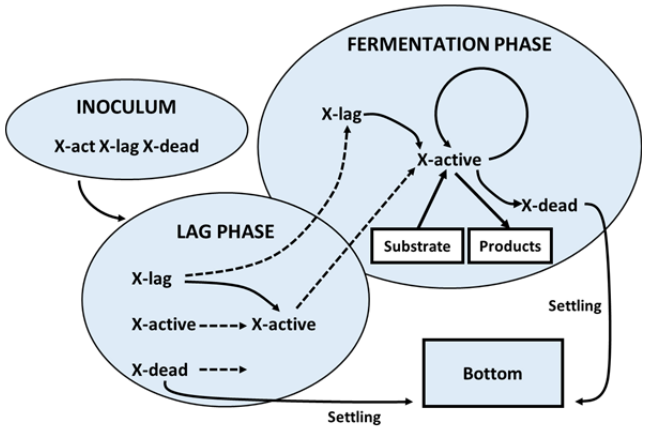

Figure 1. Kinetic model for beer fermentation under industrial conditions (de Andres-Toro, 1998).

The kinetic model of beer fermentation by de Andrés-Toro et al. (1998) has been selected for study due to its direct applicability to the industrial process:

- Published parameters are derived from a very large array of experiments, resulting in a wide temperature range (8–24 ºC) which ensures high fidelity and applicability.

- The model includes all prominent by-products which degrade beer product quality in terms of taste and aroma, rendering the model valuable for assessing performance.
- Predicted profiles indicate the highest fidelity with experimental and pilot-plant data in comparison to other models, due to successful validation against over 200 fermentations.

The 7 model state (Eqs. 1-7) trajectories are governed by temperature-dependent production and consumption factors (Eqs. 8-12); the model structure is shown in Fig. 1. Yeast cells transition from latent to active to dead over time, with only active cells able to promote fermentation (conversion of sugar to ethanol). Two by-products are considered alongside the primary reaction pathway: ethyl acetate (Eq. 5) and diacetyl compounds (Eq. 6). Diacetyl (2,3-butanedione) has a pungent butter-like aroma (Izquierdo-Ferrero et al., 1997), while ethyl acetate is often used as an indicator of esters present, having an odour similar to nail varnish remover (Hanke et al., 2010). Incorporating external heat transfer dynamics induces lag (hence online control is inoperable, due to limited instrumentation); it also increases model complexity and escapes the scope of this work, which is to explore and map optimal T(t) solution variability. No external heating is provided (yeast biocatalytic activity is an exothermic phenomenon), but jacket cooling is used in practice, in order to regulate fermentation and avoid flavour species concentration runaway.

$$\frac{dX_A(t)}{dt} = \mu_x(t,T)\cdot X_A(t) - \mu_{DT}(t,T)\cdot X_A(t) + \mu_L(t,T)\cdot X_L(t) \quad (1)$$

$$\frac{dX_D(t)}{dt} = -\mu_{SD}(t,T)\cdot X_{dead}(t) + \mu_{DT}(t,T)\cdot X_A(t) \quad (2)$$

$$\frac{dC_S(t)}{dt} = -\mu_S(t,T)\cdot X_A(t) \quad (3)$$

$$\frac{dC_E(t)}{dt} = f(t)\cdot \mu_e(t,T)\cdot X_A(t) \quad (4)$$

$$\frac{dC_{EA}(t)}{dt} = Y_{EA}(T)\cdot \mu_x(t,T)\cdot X_A(t) \quad (5)$$

$$\frac{dC_{DY}(t)}{dt} = \mu_{DY}\cdot C_S(t)\cdot X_A(t) - \mu_{AB}\cdot C_{DY}(t)\cdot C_E(t) \quad (6)$$

$$\frac{dX_L(t)}{dt} = -\mu_L(t,T)\cdot X_L(t) \quad (7)$$

$$\mu_x(t,T) = \frac{\mu_{x_0}(T)\cdot C_s(t)}{0.5\cdot C_{s_0}+C_e(t)} \quad (8)$$

$$\mu_{SD}(t,T) = \frac{\mu_{SD_0}(T)\cdot 0.5\cdot C_{s_0}}{0.5\cdot C_{s_0}+C_e(t)} \quad (9)$$

$$\mu_S(t,T) = \frac{\mu_{S_0}(T)\cdot C_S(t)}{k_S(T)+C_S(t)} \quad (10)$$

$$\mu_E(t,T) = \frac{\mu_{E_0}(T)\cdot C_s(t)}{k_E(T)+C_s(t)} \quad (11)$$

$$f(t) = 1 - \frac{C_E(t)}{0.5\cdot C_{s_0}} \quad (12)$$

A more detailed description of the model can be found in its original publication (de Andrés-Toro, 1998). The explicit nonlinear functions of all temperature-dependent model parameters which appear in Eqs. (8 - 11) have been derived via regression of industrial scale fermentation data obtained for temperature in the range of 8–24 °C, and are also summarised here in Table 1.

Table 1. Nonlinear model parameter functions of temperature, and initial conditions for beer fermentation simulation

Description	Symbol	Temperature function	Value	Units
Maximum sugar consumption rate	μ_{So}	$\exp(-41.92 + 11654.64/T)$	(variable)	h^{-1}
Maximum ethanol production rate	μ_{Eo}	$\exp(3.27 - 1267.24/T)$	(variable)	h^{-1}
Specific cell activation rate	μ_{L}	$\exp(30.72 - 9501.54/T)$	(variable)	h^{-1}
Maximum cell growth rate	μ_{xo}	$\exp(108.31 - 31934.09/T)$	(variable)	h^{-1}
Specific cell death rate	μ_{DT}	$\exp(130.16 - 38313/T)$	(variable)	h^{-1}
Maximum dead cell settling rate	μ_{SDo}	$\exp(33.82 - 10033.28/T)$	(variable)	h^{-1}
Ethyl acetate:sugar coefficient	Y_{EA}	$\exp(89.92 - 26589/T)$	(variable)	(–)
Diacetyl production rate	μ_{DY}	(Carrillo-Ureta et al., 2001)	$1.27672 \cdot 10^{-7}$	$g^{-1}\ h^{-1}\ L$
Diacetyl consumption rate	μ_{AB}	(Carrillo-Ureta et al., 2001)	$1.13864 \cdot 10^{-3}$	$g^{-1}\ h^{-1}\ L$
Initial simulation conditions	$X_{inc,0}$	Biomass inoculum (pitching rate)	4	$g\ L^{-1}$
	$(C_s)_0$	Sugar concentration	130	$g\ L^{-1}$

1.2.3 Process Targets: Objective Function

When considering what it is desirable to improve in a fermentation process there are two obvious contenders: reduced duration and heightened alcohol content (even if this requires later dilution, it is still desirable to increase yield). In addition to batch time minimisation and alcohol production maximisation, all prior authors have elected to include terms for minimisation of both by-products within their respective optimisation objective functions. However, as is known that within certain beer products the concentrations of both ethyl acetate and diactyl compounds shall be indistinguishable below certain levels, efforts towards further reduction and concentration minimisation are redundant.

As such it is deemed more appropriate to consider an objective function only seeking to minimise production time and maximise sugar conversion to ethanol (with variable relative weights) while treating the final concentrations of both ethyl acetate and diacetyl compounds as strict constraints to avoid unnecessary efforts towards further by-product reduction.

Thus the following objective shall be used in this study, considering only a terminal payoff:

$$\mathrm{J} = \min f(u) = -W_E \cdot \widetilde{C_E} - W_t \cdot \widetilde{\left(\frac{1}{t_f}\right)} \tag{13}$$

$$s.t. \qquad (C_{EA})_{t=t_f} \leq 2 \text{ ppm} \tag{14}$$

$$(C_{DY})_{t=t_f} \leq 0.1 \text{ ppm} \tag{15}$$

Here our control vector u, represents the temperature profile, T(t), for fermentation. Moreover, W_E and W_t are the respective weights of the two components in the objective function: while a large range of weight values have been investigated, for conciseness only the case W_E = 0.75 W_t = 0.25 shall be presented in this paper, which encompasses the desirable window for operation. $\widetilde{(1/t_f)}$ is the inverse batch time normalised by division with the maximum value

attained from exhaustive simulation (Rodman and Gerogiorgis, 2016) and $\widetilde{C_E}$ is the ethanol concentration normalised in the same way. In doing so the normalised ethanol concentration, $\widetilde{C_E}$ ranges from 0.68 when $C_E = 42$ g L^{-1} to 1 when $C_E = 61.3$ g L^{-1}, similarly the normalised inverse batch time, $\left(\widetilde{1/t_f}\right)$, ranges from 0.62 to 1 when t is 99 hrs and 160 hrs respectively.

Given the strong dependence of yeast health on system temperature it is necessary to include an additional constraint such that the control profile (temperature) remains within acceptable levels. Eq. 16 ensures that the lower temperature limit excludes scenarios in which the system lacks enough energy to promote cell growth while the upper limit ensures bacteria which are present above this temperature cannot thrive, while also preventing the temperature from reaching a level at which undesirably high by-product concentrations are known to be produced.

$$T(t) \in [9\ °C, 16\ °C] \text{ for all t} \in [t_0, t_f] \tag{16}$$

The problem formulation relies upon a fundamental assumption that the batch reactor features perfect mixing and ideal liquid mixture behaviour. Furthermore, we treat the reaction temperature directly as the manipulated (control) variable, assuming negligible delay between supplying or removing heat and the bulk broth temperature changing. Such an assumption can be valid on small or medium scale vessels (such those used in the booming craft beer movement in recent years), where temperature manipulations can be realised extremely quickly. Care must be taken when extrapolating to larger industrial scale vessels, where lag time can be more significant, and direct temperature control becomes less realistic.

1.3 Prior work

Since the early work of Denbigh (1958) optimal control of batch reactors has received a vast amount of research interest (Aziz and Mujtaba, 2002). Logsdon (1990) considered a maximum conversion and fixed timeframe optimisation problem for a consecutive reaction scheme. This work sought the optimal temperature profile, T(t), to maximise conversion of the desired product in a predefined reaction time, solved with a two-point collocation method. Later Logsdon and Biegler (1992) solved the same problem with a relaxed simultaneous approach requiring less CPU time to solve. Luus (1994) also considered a maximum conversion for consecutive reactions. Here the piecewise constant T(t) profile with fixed switching is optimised by iterative dynamic programming (IDP) to maximise conversion. Garcia and colleagues (1995) considered another conversion maximisation problem a consecutive parallel reaction scheme. The dynamic optimal control is discretised into an NLP problem and solved by a generalised reduced gradient method coupled with a golden search technique. The authors compared considering 5 and 10 time intervals to discretise the temperature profile, concluding that there is no significant

improvement upon increasing the discretisation density and resultant NLP problem size. Aziz and Mujtaba (2002) consider a CVP method for both maximum conversion (operation time is fixed a priori) and minimum time problems (conversion is fixed a priori) for a typical consecutive reaction scheme in batch reactors. They explore the effect of waste and/or temperature constraints (both path constraints and terminal value constraints) on the optimal operation policies and on the attainable performance (solution objective function values).

Specifically pertaining to beer fermentation, numerous authors have used the de Andrés-Toro (1998) model for optimisation studies. Several have been stochastic approaches, including genetic algorithms (Carrillo-Ureta et al., 2001), ant colony system (Xiao et al., 2003) and simulated annealing (Rodman and Gerogiorgis, 2016a). These have addressed both the single objective case for batch time minimisation or ethanol yield maximisation (de Andrés-Toro, 1998; Carrillo-Ureta, 2001), or both (Rodman and Gerogiorgis, 2016). Additionally, Bosse and Griewank (2014) have used the kinetic model to generate optimal control profiles using a sweeping dynamic optimisation methodology. The process involves guessing a control path and using this to integrate the states forward in time. This allows the costates to be integrated backwards through the process time span: a new control profile is thus deduced by maximising the Hamiltonian for all t $\in [t_0, t_f]$, and the process is repeated until path convergence is attained. The authors were able to compute a more preferable temperature profile using the same objective, compared to a prior stochastic approach (de Andrés-Toro et al., 1997).

In this paper we investigate the performance of two different dynamic optimisation strategies for batch beer fermentation temperature control optimisation. A range of initialisation solution profiles to elucidate the robustness of either strategy for batch fermentation optimisation and to observe the solution dependence on the initialisation strategy. The nonlinearity of the dynamic process model coupled with the constraints on terminal state values (Eqs 14-15) introduce non-convexity into the case study problem presented. Herein local solutions exist in the solution space, and an appropriate initialisation strategy becomes pertinent. Additionally, the bi-criteria weighted sum objective (Eq. 13) can lead to a very flat objective space due to the inherent trade-off between competing objective components which can potentially lead to convergence issues.

2. Materials and Methods

In this study we compare two different dynamic optimisation methodologies: a simultaneous strategy (CVP) with an interior point algorithm and a sequential dynamic optimisation procedure with orthogonal collocations on finite elements, complete parametrisation (CP). The algorithms used are detailed below.

2.1 Sequential Strategy for Dynamic Optimisation: Control Vector Parametrisation

The sequential approach to direct dynamic optimisation (often referred to as control vector parametrisation, CVP) involves discretising the control trajectory to a function of a few parameters, while the state equations remain in ODE/DAE form (Biegler et al., 2012). By defining a finite number of equal size piecewise segments within the temperature profile a NLP problem can be formulated for Eqs (1-16), which any one of many large scale nonlinear programing solvers may be applied. Herein function evaluations still invoke integration across the time horizon, as the state trajectories remain continuous. Both methodologies employed in this study are implemented in MATLAB 2017a on a Windows system. Integration in the CVP method is performed using the ode45 function based on an explicit Runge-Kutta (4,5) formula, the Dormand-Prince pair (Dormand, and Prince, 1980; Shampine, and Reichelt; 1997) .

2.1.1 Interior Point Algorithm

IPOPT (Interior Point Optimizer) is a leading open source software package for large-scale nonlinear optimization. It solves general nonlinear programming problems of the form:

$$\min_{x\in\mathbb{R}^n} \quad f(x) \tag{17}$$

$$s.t. \quad g^L \leq g(x) \leq g^U \tag{18}$$

$$x^L \leq x \leq x^U \tag{19}$$

where $x\in\mathbb{R}^n$ are the optimization variables (possibly with lower and upper bounds, $x^L \in (\mathbb{R} \cup \{-\infty\})^n$ and $x^U \in (\mathbb{R} \cup \{+\infty\})^n$, $f : \mathbb{R}^n \rightarrow \mathbb{R}$ is the objective function, and g : $\mathbb{R}^n \rightarrow \mathbb{R}^m$ are the general nonlinear constraints. The functions f(x) and g(x) can be linear or nonlinear and convex or non-convex. The constraints, g(x), have lower and upper bounds, $g^L \in (R \cup \{-\infty\})^m$ and $g_U \in (R \cup \{+\infty\})^m$. Equality constraints of the form $g_i(x) = \bar{g}_i$ are treated as inequality constraints with equal lower and upper bounds: $g_i^U = g_i^L = \bar{g}_i$. IPOPT implements an interior point line search filter method that detirmines a local solution of Eqs. 17-19. Details of the full mathematical algorithm can be found in several publications (Wächter, 2003; Wächter and Biegler, 2005a-b; 2006; Nocedal et al., 2009). IPOPT has been utilised via OPTI's MATLAB® implementation of the solver (Currie and Wilson, 2012) for the CVP approach in this work.

2.2 Simultaneous Strategy for Dynamic Optimisation: Complete Parameterisation

2.2.1 Dynopt for Fermentation Optimisation

The alternative direct method for dynamic optimisation (a simultaneous strategy) has also been performed in this study. Here the control trajectory is again discretised, however now the NLP problem is derived by also converting the ODE state model into algebraic equations, the coefficients of which become decision variables. This has been implemented using the Dynopt package (Cizniar et al., 2006) to compute the nonlinear programming problem. Orthogonal

collocations on finite elements are used to parameterize the ODE system (process model) to algebraic equations to formulate the NLP problem: both control and state profiles are approximated by a combination of basis functions. The methodology approximates the solution with Lagrange polynomials over each element, *i*:

$$x_{K_x}(t) = \sum_{j=0}^{Kx} x_{ij}\Phi_j(t), \qquad \Phi_j(t) = \prod_{k=1,j}^{Kx} \frac{t - t_{ik}}{t_{ij} - t_{ik}} \tag{20}$$

$$x_{K_u}(t) = \sum_{j=0}^{Ku} u_{ij}\,\theta_j(t), \qquad \theta_j(t) = \prod_{k=1,j}^{Ku} \frac{t - t_{ik}}{t_{ij} - t_{ik}} \tag{21}$$

Where x_{K_x} is a piecewise polynomial of order $Kx + 1$, u_{K_x} is a piecewise polynomial of order Ku. Figure 2 is representative of orthogonal colocation with 1 collocation point per control segment (piecewise constant), and 3 collocation points for each state trajectory element. This polynomial form allows the bounding of both the states and control trajectories, enabling path constraints to be imposed on the temperature profile in the problem formulation (Eq. 16).

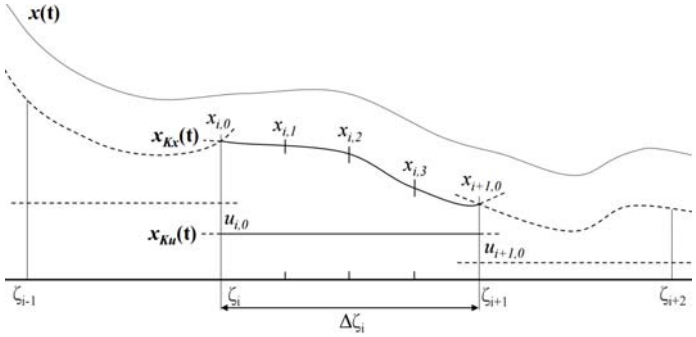

Figure 2. Collocation method for state and control profiles (adapted from Cizniar et al., 2006 & Biegler, 2010)

The NLP formulation now consists of the ODE model (Eqs. 1 - 7) discretised on finite elements, continuity equations for state variables and the inequality constraints on the system (Eqs. 14 - 15), and is compatible with the interior point NLP solver described in Section 2.1.

3. Results and Discussion

3.1 Sequential Optimisation

3.1.1 Piecewise Constant Control Profiles

Profiles which are piecewise constant between discreet time points are first computed to investigate the performance of the algorithm and its sensitivity to the input initial guess (initialising solution, T_0), and as to how performance is affected by varying the degree of discretisation (N). To achieve this a range of cases are systematically considered: four discretisation levels have been considered: N = [6, 12, 18, 24] along with four isothermal initialising solutions: T_0 (°C) = [11, 12, 13, 14], producing 16 permutations to be solved in turn.

The optimal profile computed in each case is shown in Fig. 3, with the performance criteria from each case shown in Fig. 4 using MATLABs fmincon solver (Waltz et al., 2006), using objective weights $W_t = W_E = 0.5$ and a fixed terminal time. Batch time is this defined as the tome to consume 99.5% of the feed sugars. The equivalent results are also shown in Fig. 5-6, here using IPOPT and $W_t = 0.25$ and $W_E = 0.75$.

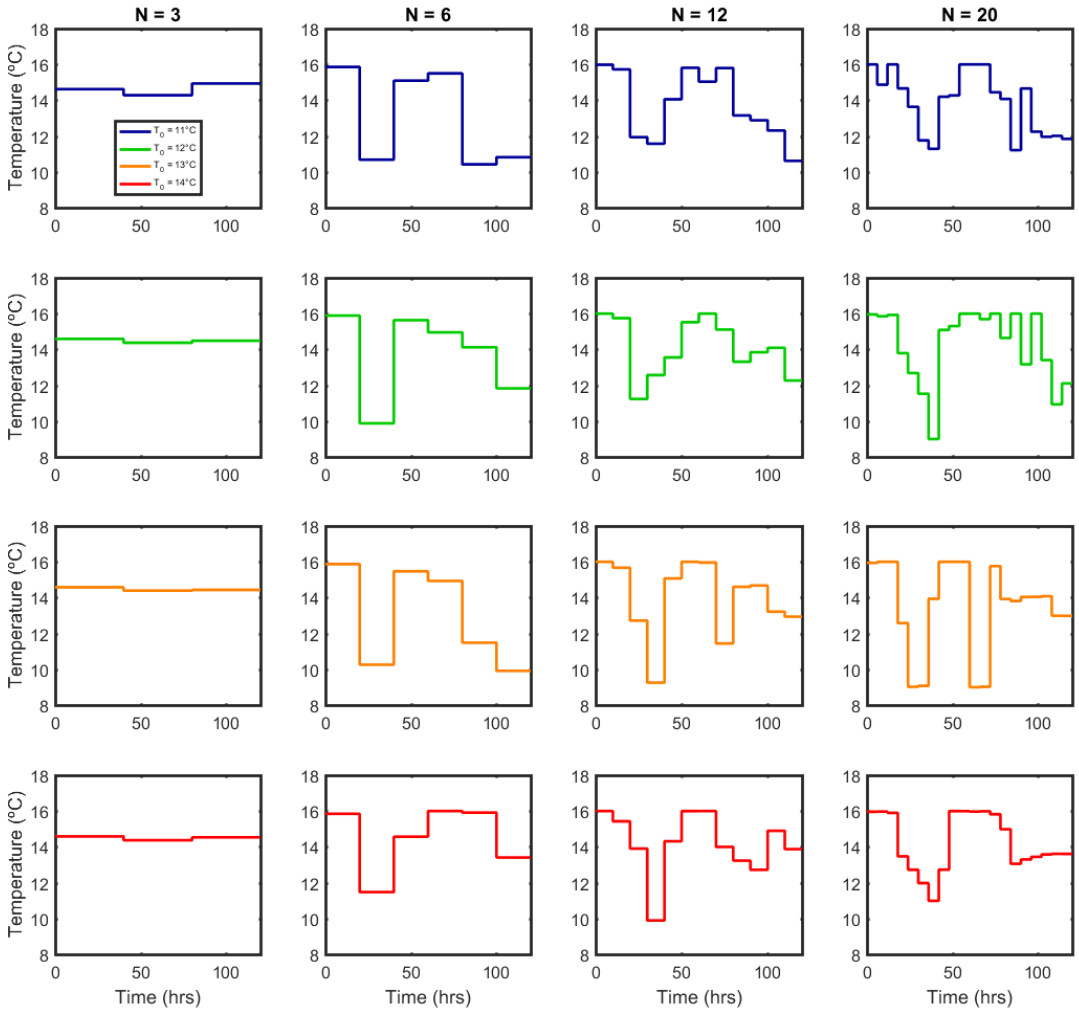

Figure 3. Piecewise constant T(t) solutions – CVP with fmincon & fixed endpoint, $W_t = W_E = 0.5$.

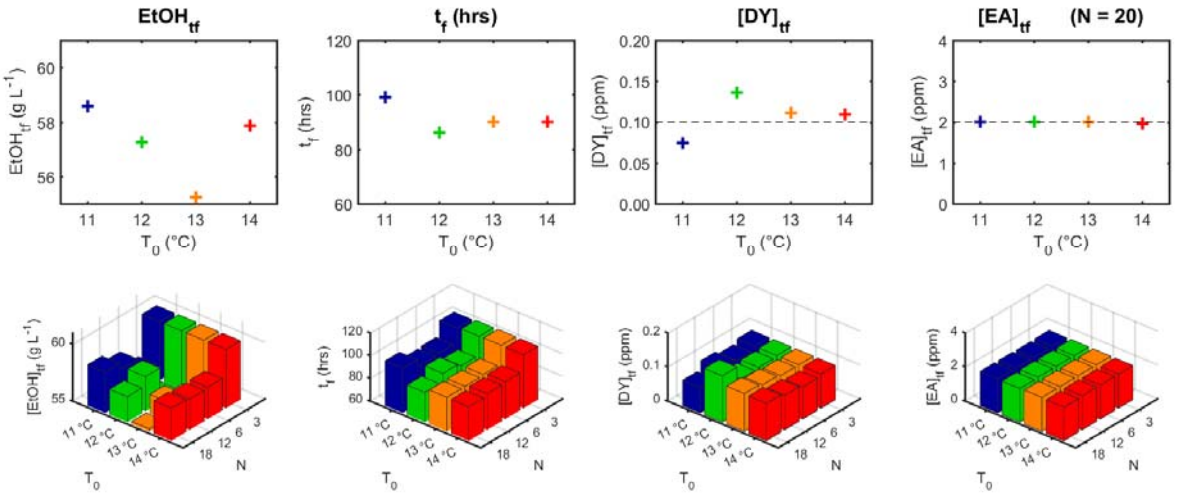

Figure 4. Influence of discretisation level (N) and initialising isothermal profile (T_0) on piecewise constant profile performance - CVP with fmincon & fixed endpoint.

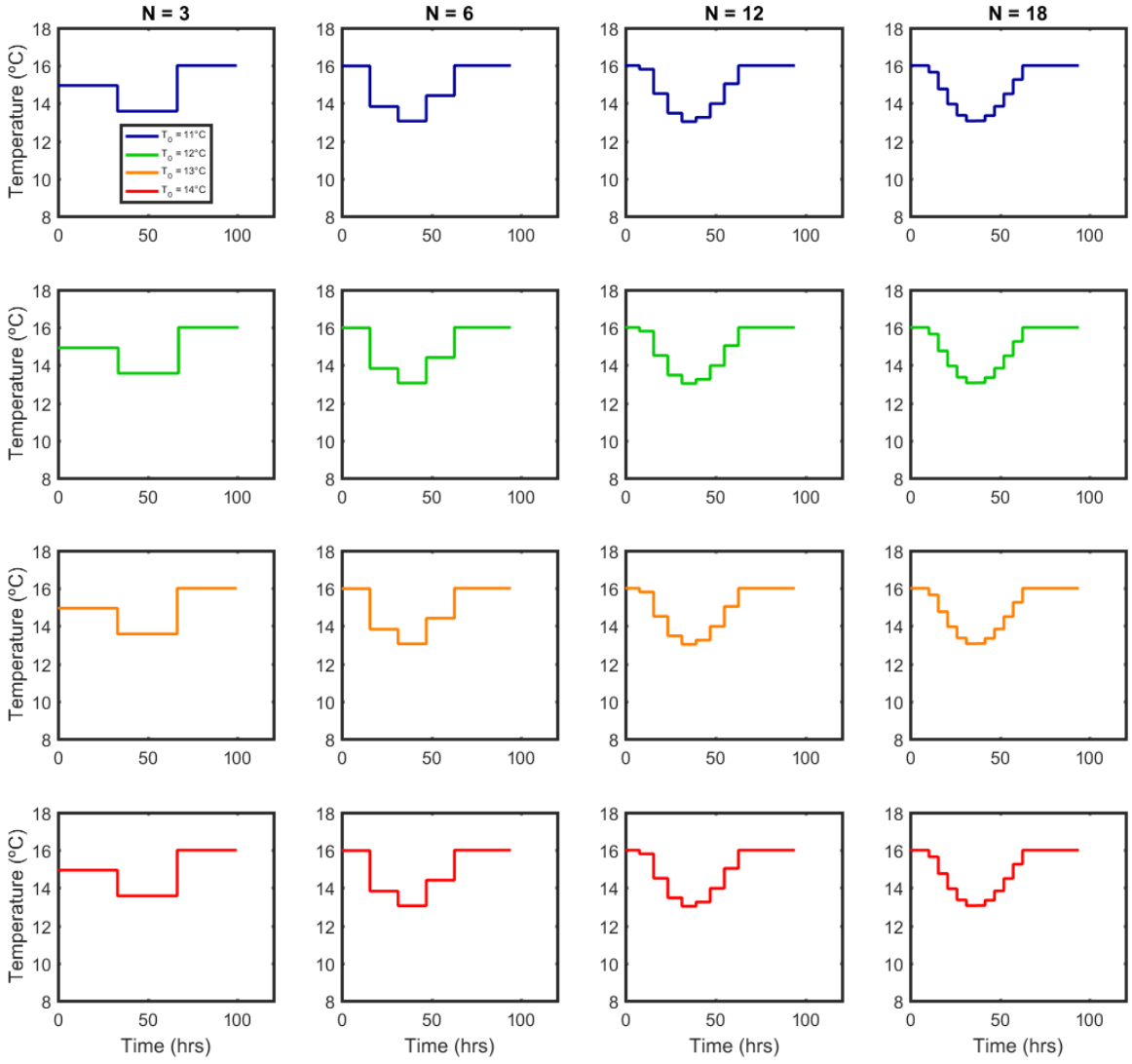

Figure 5. Piecewise constant T(t) solutions – CVP with IPOPT & moving endpoint, $W_t = 0.25$, $W_E = 0.75$.

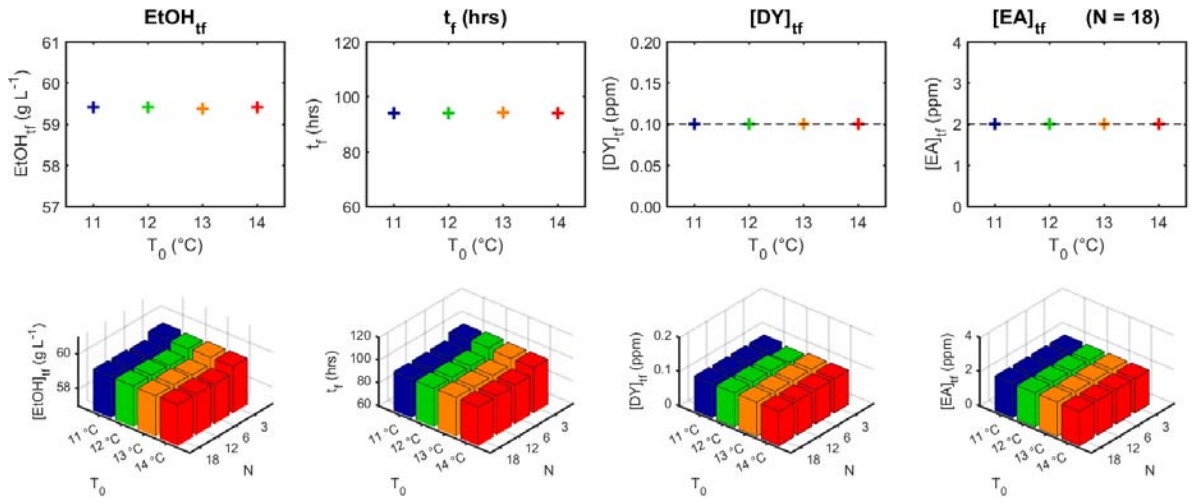

Figure 6. Influence of discretisation level (N) and initialising isothermal profile (T_0) on piecewise constant profile performance – CVP with IPOPT and moving endpoint.

3.1.1.1 Effect of Initialising Temperature Profile

Computed optimal control profiles on an identically discretised T(t) domain for numerous initialising temperature profiles can be seen in each column in Fig. 5. From top to bottom isothermal profiles at 11, 12, 13 and 14 °C were used for the initial iteration respectively. The performance of each solution obtained with IPOPT is tabulated in Table 2.

It is observed that the same general solution form is produced in all cases presented from this method. This tends initially to the highest permitted temperature for the first stages of the process (16 °C) to accelerate the yeast growth and promote fermentation immediately. This is followed by a gradual dip in temperature down to 13 °C, before climbing back to 16 °C in parabola form over hours 10-70. This acts to prolong the maximum yeast concentration and delay cell death, permitting accelerated fermentation.

It is shown here that the solution produced for the optimal control profile problem is not particularly dependent on the choice of input profile when utilising this CVP methodology. For all four discretisation levels (N = 3-18) the solution produced is identical, indicating independence to the initialisation profile among those trailed, suggesting local solutions have not been encountered by the NLP algorithm towards converging to this robust T(t) solution profile.

3.1.1.2 Effect of increasing time domain discretisation.

To access the effect of increasing the discretisation level of the control profile, the computed results for N = 3, 6, 12 and 18 (representing the number of equispaced time segments in which the fermenter temperature is piecewise constant) are shown in each row of Fig. 5 for a specific initialising isothermal temperature.

For the lowest levels of discretisation (N = 3, 6) significant differences are seen in the form of the computed profiles, showing that for course discretisation's the solution form is dictated by the size of the time segments within the profiles. When N = 3 the optimal scenario involves little temperature variation with only a very minor decrease in the middle portion, with and greater decrease not being effective as it would be sustained for longer than desirable. Once N = 6 the shorter time segments mean that it is now possible to drop the temperature more significantly for a shorter period of time, which is more desirable in this case due to acting to suspend the cell death rate. Increasing N further to 12 allows the solution form to develop further: more gradually decreasing the temperature towards the end of the process permits the by-product concentrations to be reduced while maintain an adequate fermentation rate.

The last case (N = 18) shows refinement upon the case when N = 12, with no significant change in solution form. Improvements in objective function value are less significant, suggesting that optimality is being approached for the specific objective. A trade off exists as the required CPU time for computing the profiles increases rapidly with increasing discretisation level suggesting little value in increasing discretisation beyond this point.

It is noteworthy that the majority of profiles produced from CVP with an interior point method are not highly changeable in form: that is to say there is minimal abrupt changes in temperature so no secondary smoothing procedure is required, which often the case with stochastic techniques (Carrillo-Ureta et al., 2001; Xiao et al., 2004) which often computed abrupt changes in the control profile which would not be attainable in a real world application.

3.1.1.3 Control Profile Performance

The upper row in Fig. 6 compares the performance of the profiles computed for N = 18 with each initialising isothermal profile considered. The second row of plots in Fig. 4 considers a third axis to simultaneously visualise the effect of both discretisation level and initialising profile on the resulting fermentation performance. These results produced with IPOPT demonstrate effective independence to the initialisation profile and the discretisation level, once N is increased past 6.

In contrast Fig. 4 shows how the results produced with fmincon are highly variable. It is observed that the ethanol concentration actually decreases when N is increased for all values of T_0. In contrast the batch time decreases consistently with increasing N for all values of T_0: batch time decreases much more rapidly that ethanol concentration with increasing N, such that the overall objective value continues to improve with greater discretisation. This result suggests that the ethanol concentration of the product may have too little weighting in the objective (Eq. 13) as it is being consistently sacrificed as to improve the overall objective value. It is noteworthy

that between N = 12 and N = 20 there is significant change in both ethanol concentration and batch time for any single T_0, showing that the solution performance is still dependant on the discretisation level. It would be beneficial to continue to increase N until no significant further improvement is found, meaning that a discretisation level independent soliton has been obtained. The product concentrations of undesirable fermentation by-products are shown in the right half of figure 4. It is apparent that the ethyl acetate concentration constraint (Eq 14) is universally fulfilled, however the constraint imposed on the diacetyl concentration (Eq 15) has been regularly violated when N = 20. The algorithm has converged at unfeasible solutions due to not being able to fulfil the imposed constraint the objective, rendering their little reason to progress to higher values of N.

3.1.2 Piecewise Linear Control Profiles

It is apparent that such instantaneous temperature gradients as shown in Fig. 3 and 5 are not attainable in large scale process equipment. Piecewise linear profiles are computed using the same methodology, as to see how these more readily implementable solutions compare to the more simple piecewise constant profiles in section 3.2, and if the additional degrees of profile freedom will enable constraint satisfaction across the range of N and T_0 considered.

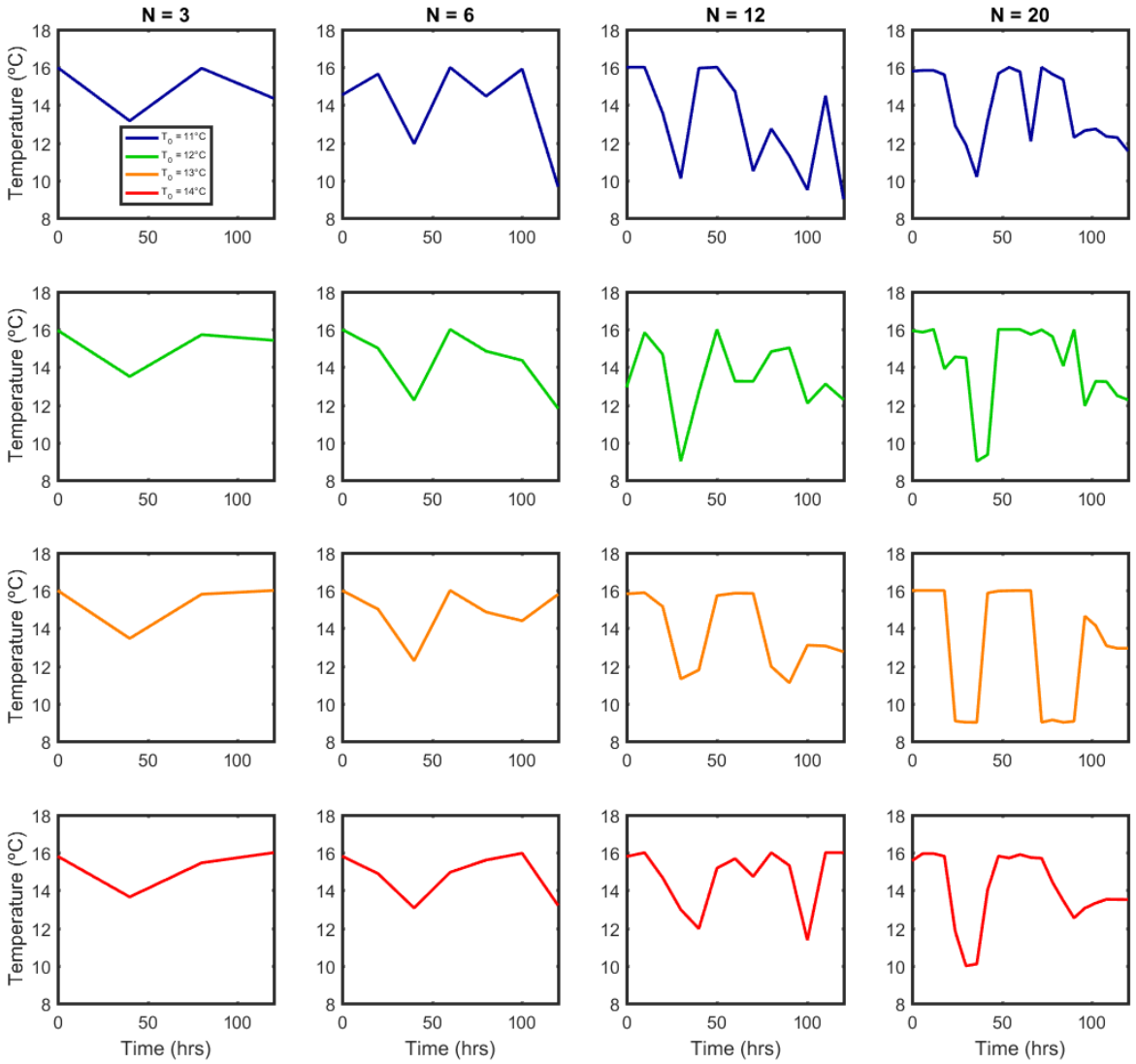

Figure 7. Piecewise linear T(t) solutions – CVP with fmincon & fixed endpoint, $W_t = W_E = 0.5$.

The same 16 cases have been solved in turn: N = [3, 6, 12, 20], T_0 (°C) = [11, 12, 13, 14], the optimal profile computed in each case is shown in Fig. 5, with the performance criteria from each case shown in Fig. 6.

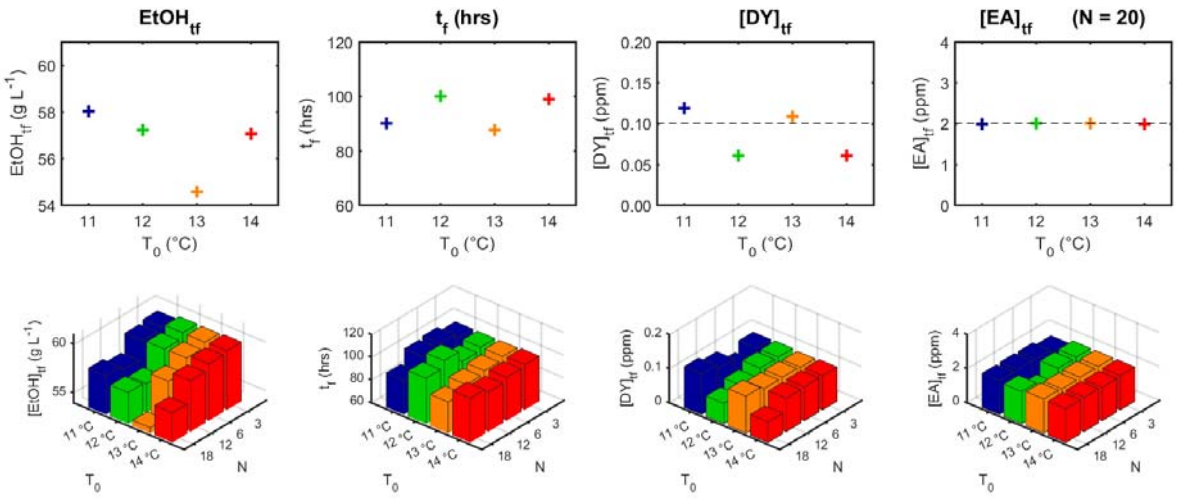

Figure 7. Influence of discretisation level (N) and initialising isothermal profile (T_0) on piecewise linear profile performance - CVP with fmincon & fixed endpoint.

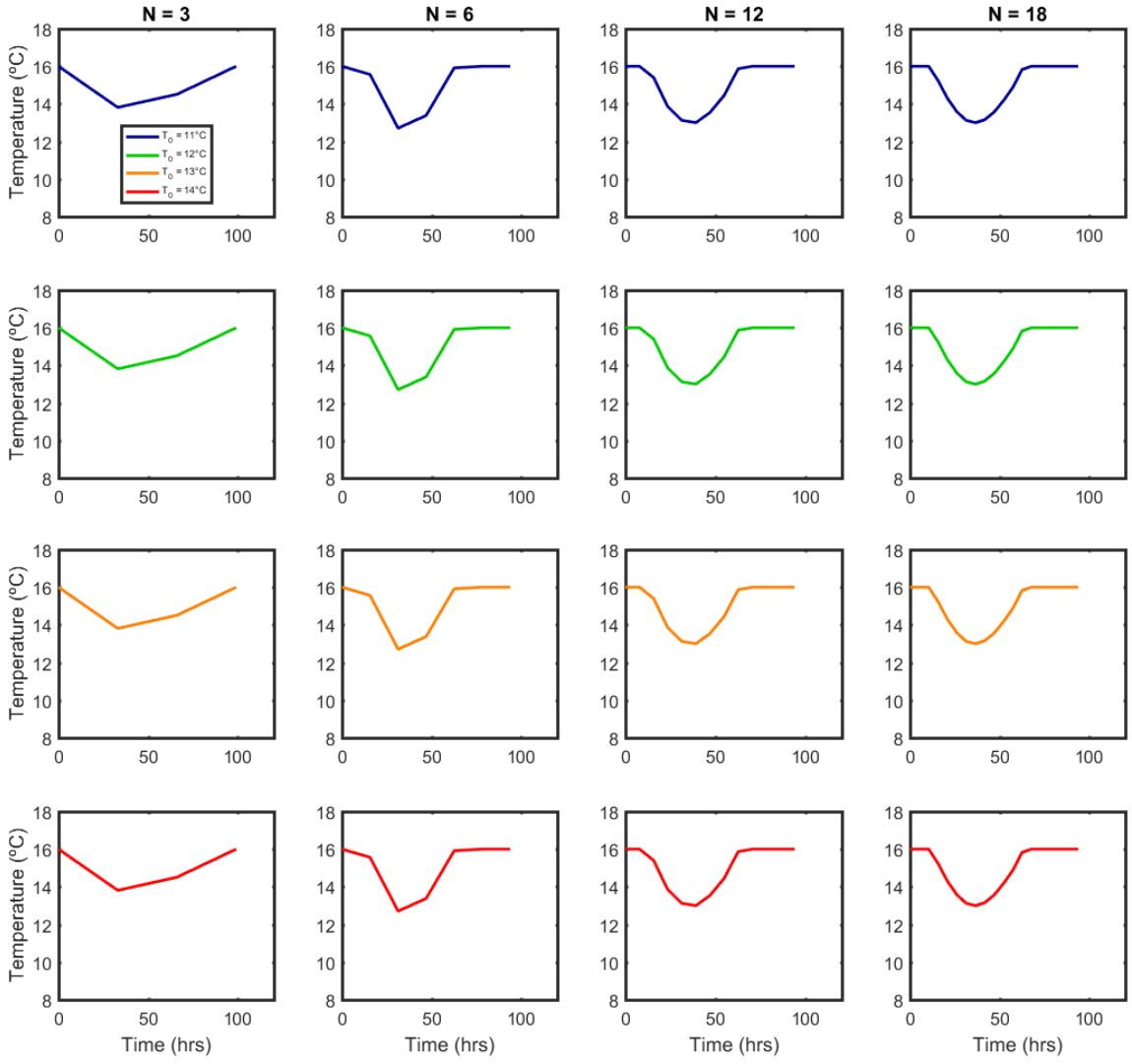

Figure 8. Piecewise linear T(t) solutions – CVP with IPOPT & moving endpoint, $W_t = 0.25$, $W_E = 0.75$.

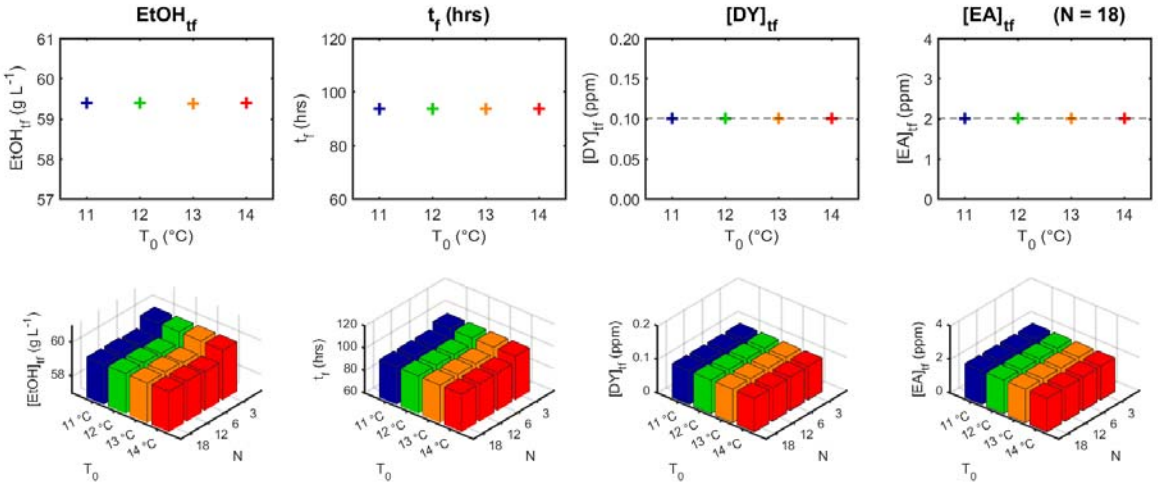

Figure 9. Influence of discretisation level (N) and initialising isothermal profile (T_0) on piecewise linear profile performance - CVP with IPOPT & moving endpoint.

Comparing Fig. 7 to Fig 3 shows how the profiles differ for equivalent N and T_0 between piecewise linear and piecewise constant. It can be seen that the profile forms are extremely similar, with intermediate cooling prevailing as a strategy for optimal fermentation performance. For the lowest discretisation level studied (N = 3), rather than producing an approximately isothermal profile as in the piecewise constant cases, a dip has been introduced which improves the objective greatly. Once N = 6 this dip can become more pronounced and sustained for a lesser period of time, further improving the objective. As N is increased to 12 then to 20 the objective continues to improve, however as with the piecewise constant cases, it is found that the initialising solution has a significant bearing on the computed profile: when N = 20 the five profiles computed have major differences.

It is shown in Fig. 7 that the objective has improved when compared to the equivalent piecewise linear profiles due to the additional path freedom introduced. Again it is found that both batch time and ethanol concentration vary considerably with the differing profiles produced with each T_0 input. Similarly it is again shown that while the ethyl acetate constraint (Eq. 14) is satisfied, the diacetyl constraint (Eq. 15) has been violated in several cases. It is shown in Fig. 7 that as N is increased the ethanol concentration decreases, however this is alongside a reduction in batch time, representing an overall improvement in the objective. The exception to this is the case initialised with an isothermal profile of T_0 = 12 °C: it is shown that batch time actually increases in this case when the discretisation level is increased.

Again in contrast, results from IPOPT do not show such sensitivity to initialisation, with the profiles presented in Fig. 8 very closely resembling those in Fig. 5, with the benefit of being more readily implementable due to the lack of instantaneous temperature manipulations.

Table 2. Solution performance for all results produced via IPOPT.

Figure	Optimisation Method	N	Initialisation Profile	J	EtOH (g/L)	tf (hrs)	EA	DY
5	CVP PW Constant Isothermal T0	3	11 °C	-0.980	59.70	99.56	2.00	0.10
		6		-0.989	59.32	94.22	2.00	0.10
		12		-0.990	59.38	93.97	2.00	0.10
		18		-0.991	59.40	93.87	2.00	0.10
		3	12 °C	-0.976	59.64	100.66	1.98	0.09
		6		-0.989	59.32	94.22	2.00	0.10
		12		-0.990	59.38	93.97	2.00	0.10
		18		-0.991	59.40	93.87	2.00	0.10
		3	13 °C	-0.980	59.70	99.56	2.00	0.10
		6		-0.989	59.32	94.22	2.00	0.10
		12		-0.990	59.38	93.97	2.00	0.10
		18		-0.991	59.40	93.87	2.00	0.10
		3	14 °C	-0.980	59.70	99.56	2.00	0.10
		6		-0.989	59.32	94.21	2.00	0.10
		12		-0.990	59.38	93.97	2.00	0.10
		18		-0.991	59.40	93.87	2.00	0.10
8	CVP PW Linear Isothermal T0	3	11 °C	-0.984	59.96	98.99	2.00	0.10
		6		-0.990	59.32	93.78	2.00	0.10
		12		-0.991	59.40	93.80	2.00	0.10
		18		-0.991	59.39	93.73	2.00	0.10
		3	12 °C	-0.984	59.96	98.99	2.00	0.10
		6		-0.990	59.32	93.78	2.00	0.10
		12		-0.991	59.40	93.80	2.00	0.10
		18		-0.991	59.39	93.73	2.00	0.10
		3	13 °C	-0.984	59.96	98.99	2.00	0.10
		6		-0.990	59.32	93.78	2.00	0.10
		12		-0.991	59.40	93.80	2.00	0.10
		18		-0.991	59.39	93.73	2.00	0.10
		3	14 °C	-0.984	59.96	98.99	2.00	0.10
		6		-0.990	59.32	93.78	2.00	0.10
		12		-0.991	59.40	93.80	2.00	0.10
		18		-0.991	59.39	93.73	2.00	0.10
11	CP PW Constant Isothermal T0	6	11 °C	-0.988	59.33	94.49	2.01	0.10
		12		-0.990	59.53	94.66	2.11	0.11
		18		-0.991	59.38	93.70	2.00	0.10
		24		-0.991	59.36	93.65	2.02	0.10
		30		-0.991	59.34	93.71	1.99	0.10
		36		-0.991	59.37	93.68	2.00	0.10
		6	12 °C	-0.990	59.34	93.90	1.99	0.10
		12		-0.991	59.40	93.73	2.01	0.10
		18		-0.991	59.39	93.73	2.00	0.10
		24		-0.991	59.40	93.71	2.00	0.10
		30		-0.991	59.40	93.75	2.01	0.10
		36		-0.991	59.38	93.66	1.98	0.10
		6	13 °C	-0.989	59.32	94.12	1.99	0.10
		12		-0.991	59.35	93.81	1.99	0.10
		18		-0.991	59.37	93.70	1.98	0.10
		24		-0.992	59.41	93.60	2.01	0.10
		30		-0.991	59.39	93.70	1.99	0.10
		36		-0.991	59.38	93.78	1.99	0.10
		6	14 °C	-0.990	59.35	93.95	1.96	0.10
		12		-0.991	59.40	93.74	2.01	0.10
		18		-0.991	59.40	93.73	2.02	0.10
		24		-0.992	59.42	93.75	2.04	0.10
		30		-0.992	59.43	93.70	2.02	0.10
		36		-0.992	59.42	93.68	2.00	0.10
17	CP PW Constant Novel T0	6	A	-0.990	59.41	93.68	2.00	0.10
		12		-0.990	59.32	93.72	2.00	0.10
		18		-0.991	59.38	93.89	2.01	0.10
		24		-0.990	59.29	93.86	1.99	0.10
		30		-0.991	59.33	93.69	1.98	0.10
		36		-0.991	59.38	93.71	2.00	0.10
		6	B	-0.991	59.40	93.74	2.03	0.10
		12		-0.991	59.40	93.73	1.99	0.10
		18		-0.991	59.42	93.80	2.04	0.10
		24		-0.991	59.36	93.65	2.03	0.10
		30		-0.991	59.38	93.70	2.00	0.10
		36		-0.991	59.41	93.74	2.00	0.10
		6	C	-0.990	59.34	94.06	2.05	0.10
		12		-0.991	59.36	93.79	2.00	0.10
		18		-0.992	59.44	93.72	2.05	0.10
		24		-0.991	59.38	93.75	2.05	0.10
		30		-0.992	59.41	93.69	2.03	0.10
		36		-0.991	59.37	93.67	1.99	0.10
		6	D	-0.989	59.13	93.27	1.94	0.10
		12		-0.991	59.34	93.73	1.99	0.10
		18		-0.990	59.32	93.77	2.02	0.10
		24		-0.992	59.34	93.36	2.13	0.10
		30		-0.991	59.35	93.52	2.04	0.10
		36		-0.991	59.37	93.71	1.99	0.10

3.2 Simultaneous Optimisation Results

The optimisation problem defined by Eqs (1-15) has been solved using Dynopt (Cizniar et al., 2006). In this study the fmincon function from MATLAB has been used to solve the resultant NLP problem produced from Dynopt, using the interior point algorithm from the optimisation toolbox. This is repeated using IPOPT and providing analytical gradients for comparison. Three collocation points have been used for state trajectories, with one collocation point being used for control profiles, resulting in the computation of profiles which are piecewise-constant. For a fixed level of discretisation, N, segment length has been treated as a decision variable, meaning that profile time segments are no longer of fixed length, $\frac{t_{max}}{N}$.

3.2.1 Isothermal Initialisation

Initially, using all base case conditions for process inputs (Table 1) the methodology described here has been used to formulate control profiles for 6 levels of temporal domain discretisation (N = [3, 6, 12, 20, 30, 40] along with five isothermal initialising solutions, T_0 (°C) = [11, 12, 13, 14], producing 24 permutations to be solved in turn.

Computed optimal control profiles for numerous initialising temperature profiles and discretisation levels can be seen in each column in Figure 10. From top to bottom isothermal profiles at 11, 12, 13 and 14 °C were used for the initial simulation respectively. Comparing Fig. 10 (simultaneous) with Fig. 3 (sequential) shows the differing profile forms favoured by the two methods. The differences are drastic: the sequential (CVP) profiles show a very drastic temperature reduction around the active cell concentration maxima, meanwhile the results obtained from DynOpt (CP) favour a far less significant temperature reduction during this stage. It is remarkable that, excluding the numerous cases of constraint violation, the performance of the profiles produced by the two methods have performance which is not drastically different, despite the significant differences in their form.

3.2.1.1 Effect of initialising temperature profile.

An immediate observation from Fig. 10 is that solutions have not, meaning that globally optimality is never achieved, rather the input initialising profile has significant impact on the profile output for any set of conditions when using this methodology. This is not the case when IPOPT with analytical first derivatives are used, shown in Fig. 11. Here the T(t) solution profiles all tend to the same solution form, identical to that produced from CVP (Fig. 6).

Firstly considering the lowest level of discretisation (first column, N = 3): Using 11 °C as the initial solution allowed the algorithm to rapidly achieve the temperature profile shown in dark blue. The first 40 hours of the fermentation are carried out at approximately 15 °C, the following

40 hours use a lower temperature around 14 °C before increasing marginally to around 14.5 °C for the final 40 hours. Similarly, the light blue profile below shows the same form when initialising at 12 °C; with a greater temperature in the final third of the process (16 °C). The three remaining cases (T_0 = 13 and 14 °C) have produced a profile form differing from the aforementioned two. Here there is a gradually decreasing temperature over the three segments. It is apparent from the respective objective function values that the profile form in the latter three cases is preferable It is shown by the relatively low objective function values in all cases where N = 3 that such a low level of discretisation does not permit sufficient control over the process for an effective fermentation.

In the second column (N = 6) there is again distinct differences in the profile forms when comparing the first two cases to the later 3. The cases initialised with 11 and 12 °C favour increasing the temperature to a prolonged peak before dropping it back down, while the other three cases again prefer a general temperature decrease for the process duration. It is found that the top two cases require both longer batch times and are producing lesser ethanol, continuing the trend that these initialising solutions are resulting in less useful control profiles being computed.

The third column (N = 12) shows similar results for the first 4 initialising profiles: a gradual temperature increase takes place, and is followed by a subsequent temperature decrease. The next discretisation level (N = 20) again shows similar behaviour. The first row (T_0 = 11 °C) shows a very sporadic profile which results in poor fermentation performance, while the middle three cases all show comparable, moderate performance.

The industrial practicalities of fine manipulations to the temperature of the bulk vessel contents should be noted. While the large batch fermenters used for industrial scale brewing are capable of accurately regulating temperature, temperature gradients inevitably exist and manipulations $<$ 0.5 °C likely lie within the unavoidable variation present throughout the tank, having implications on the accuracy of model predictions.

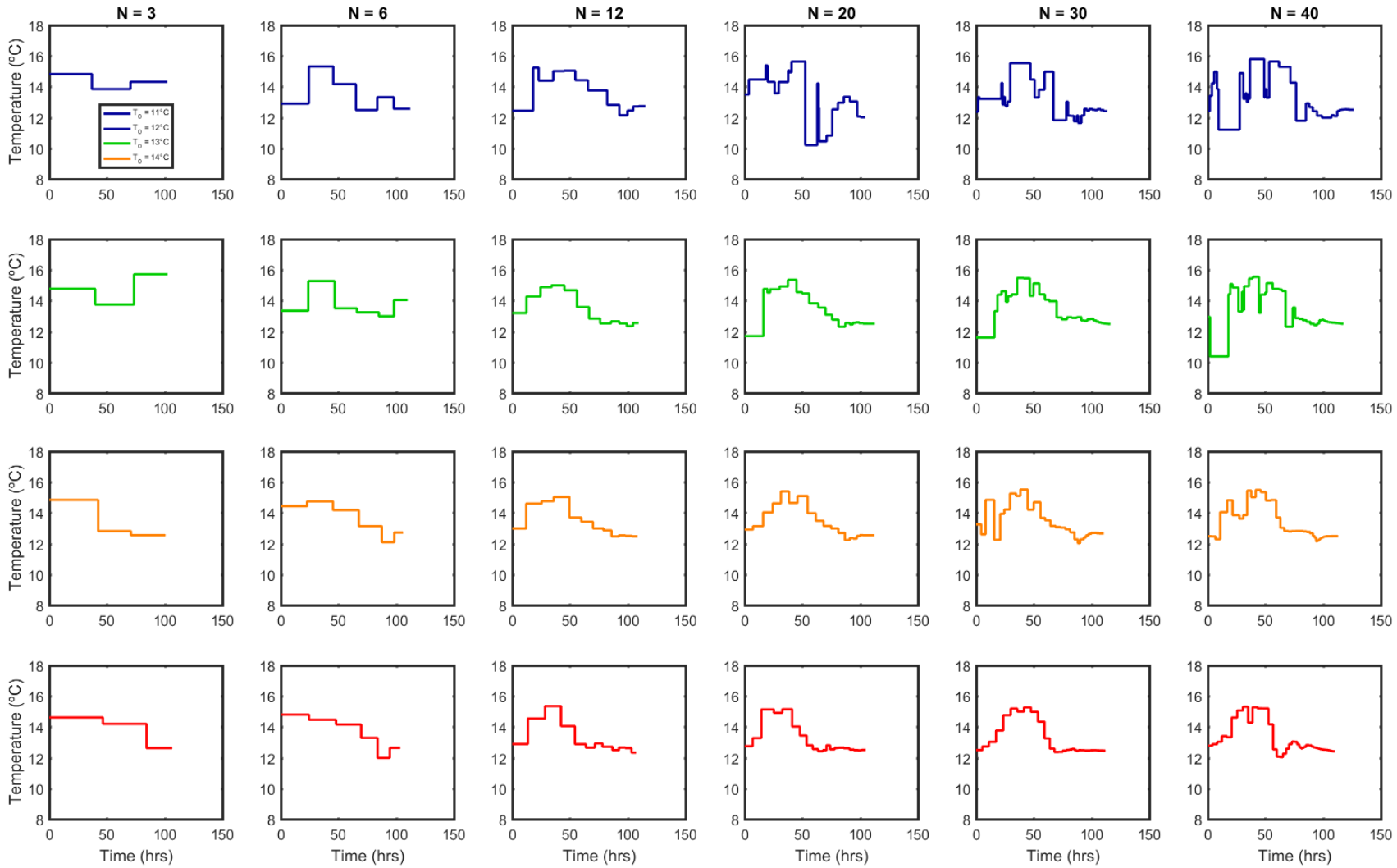

Figure 10. T(t) solutions from CP with fmincon and finite difference derivatives, for various isothermal initialisations (T_0) and discretisation levels (N), $W_t = 0.5$, $W_E = 0.5$.

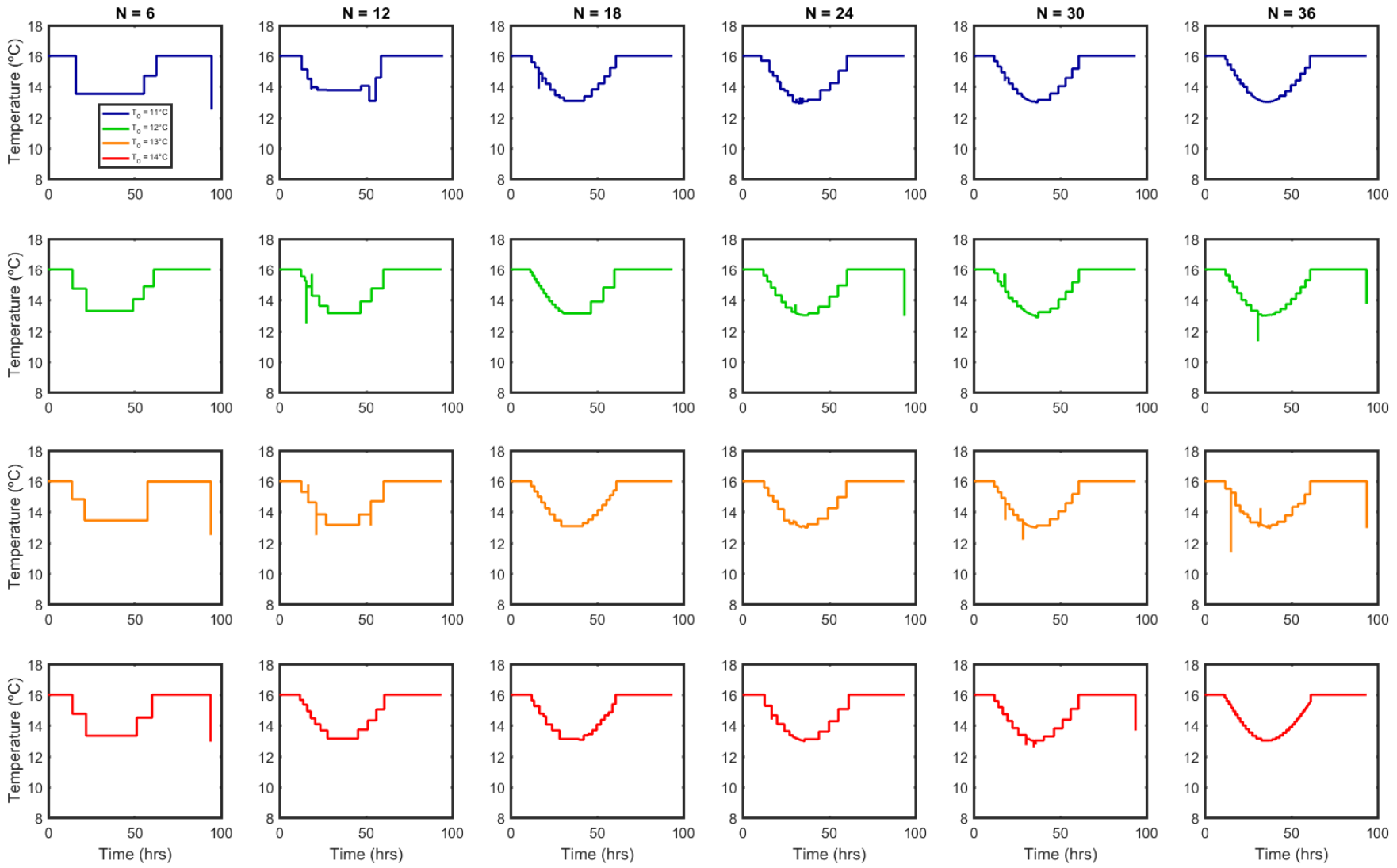

Figure 11. T(t) solutions from CP with IPOPT and analytical first derivatives, for various isothermal initialisations (T_0) and discretisation levels (N), $W_t = 0.25$, $W_E = 0.75$.

3.2.1.2 Effect of increasing time domain discretisation.

To access the effect of increasing the discretisation level of the control profile, the computed results for N = 3, 6, 12, 20, 30 and 40 (representing the number of time segments in which the fermenter temperature is piecewise constant) are shown in each row of Fig. 10 for a specific initialising isothermal temperature. Excluding the first two rows, due to the sporadic profiles computed at high N, the remaining three cases all show that as N increases the profile form develops gradually towards an optimal scenario. The preferable profile form appears to be a gradual temperature increase occurring towards a dipped peak to prolong the maximum active cell concentration, followed by a gradual temperature decrease back to around 13 °C at the end of the process.

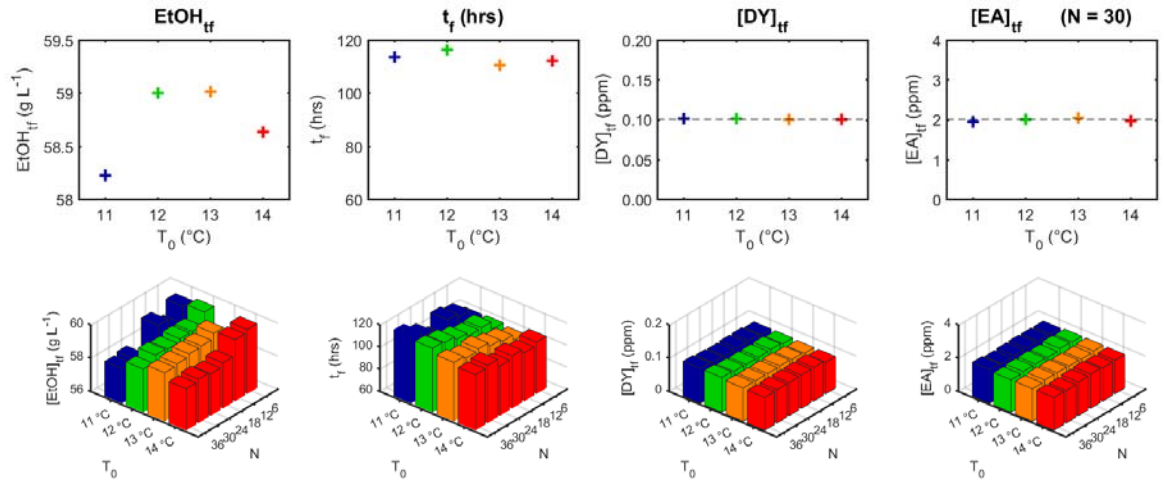

Figure 12. Influence of discretisation level (N) and initialising isothermal profile (T_0) on piecewise linear profile performance - CP with fmincon.

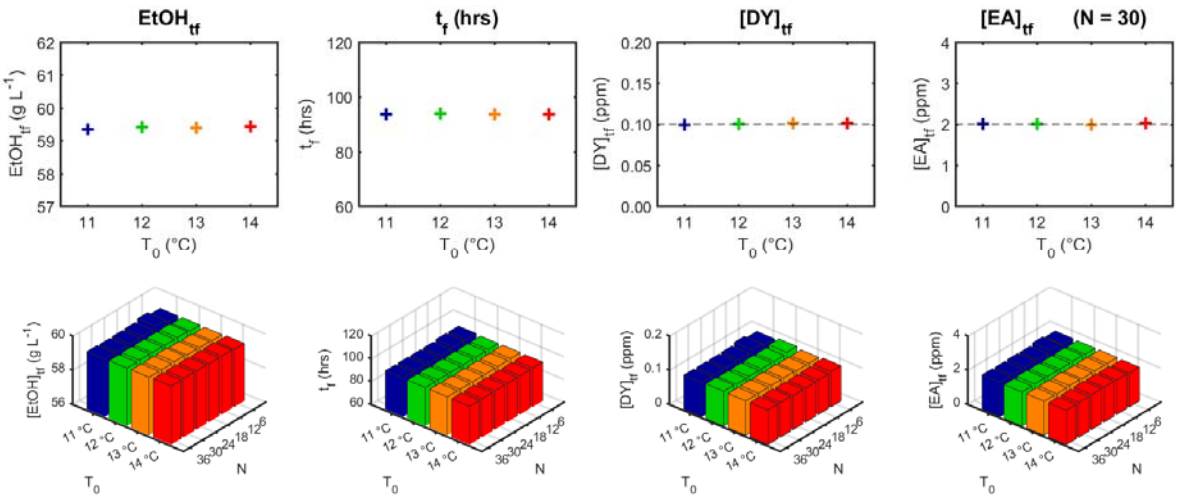

Figure 13. Influence of discretisation level (N) and initialising isothermal profile (T_0) on piecewise linear profile performance - CP with IPOPT.

3.2.1.3 Control Profile Performance

The upper row in Fig. 12 compares the performance of the profiles computed for N = 42 with each initialising isothermal profile considered. Firstly, the left most plot shows the product ethanol concentration: while a range of values are attained with varying T_0 this range is a lot narrower than for the results obtained via CVP (Fig. 3). The next plot shows the batch time achieved by the 5 profiles where N = 40: the difference of up to 18 hours is very significant showing the vast difference between the objective value obtained in these cases and the solver sensitivity to T_0. The next two plots show the by-product concentrations in the product, where it is clear that no constraints have been violated, a significant improvement over the CVP results in section 4.

The second row of plots in Fig. 12 considers a third axis to simultaneously visualise the effect of both discretisation level and initialising profile on the resulting fermentation performance. It is found that ethanol concentration decreases with increased N, and while batch time is generally reduced there are several outliers showing poor performance. This occurs when T_0 = 11 °C, likely a fragment of the initial guess (initialising solution, T_0) lying far from the optimal path, hindering attainment of a desirable solution.

3.2.2 Initialisation with Promising Candidate Profiles

Initialising with isothermal profiles may be seen as assessing the blind performance of the optimisation strategies. This can be seen as highly beneficial not only in assessing the algorithm performance, but also prevents narrowing of the attainable solution space by starting in the vicinity of local solutions. It is however shown that for the beer fermentation problem the solutions produced from isothermal initialisations, specifically when using fmincon, are of limited applicability, due to their highly changeable nature. It is now desirable to take solutions already showing promise, and see how the optimisation algorithms perform, and of the output profile solutions are more suitable for industrial manipulation.

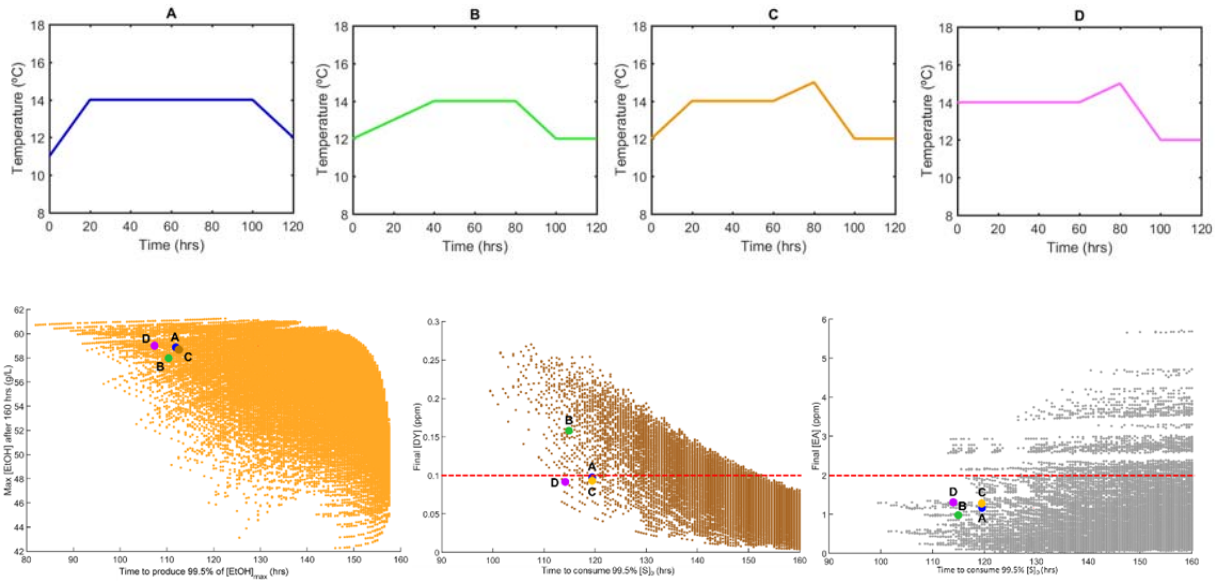

Figure 14. Performance of four promising profiles with respect to by-product concentration thresholds.

We have selected a range of profiles from a prior exhaustive simulation campaign (Rodman & Gerogiorgis, 2016a-b) performed with a low discretization level, N = 6. To visualise how these profiles perform the three lower plots indicate the position of these points within performance plots for the entire solution set. The top plot (ethanol vs. batch time) shows that the four profiles taken forward from exhaustive simulation for initialising the simultaneous optimisation procedure all fall towards the more desirable portion of the plot.

As these initialising profiles are piecewise linear and DynOpt is computing piecewise constant temperature profiles it is necessary to approximate the profiles in Fig. 9 to a piecewise constant form, which will differ for each discretisation level solved. This approximation is performed by averaging the temperature over N steps of equal duration: this transformation is shown in Fig. 15 for profile D. It is demonstrated that N increases the profile tends to the original piecewise linear form. The resulting solution profiles are presented in Fig. 16 - 17 following initialisation with the 4 candidate profiles shown in Fig. 14 for 6 discretisation levels.

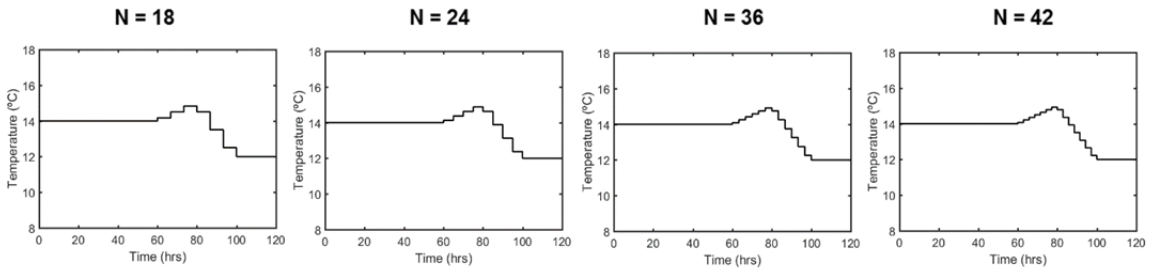

Figure 15. Piecewise constant approximations of profile D (Fig. 9) for varying discretisation levels.

3.2.2.1 Effect of increasing time domain discretisation.

Similarly to the isothermal initialisations, the profiles obtained with IPOPT and analytical first derivatives converge to the same solution trajectory, irrespective of the discretisation level or initialisation. In contrast the fmincon results (Fig. 16) show far greater dependence, as discussed below. It is shown that that regardless of the discretisation level the solution form is often similar for each initialisation profile: in general, as N increases the profile becomes refined, following a similar trajectory in a smoother manner. There are however instances where considerable deviations occur. The upper row of Fig. 16 (input profile A) shows that depending on the discretisation level, the solution profile has a drastically different initial temperature, T(t=0), ranging from 11 to 16 °C. A similar observation can be made from the third row of the same figure (input profile C). For input profile C some more drastic changes are observed as N increases. Initially, as with all cases, a single minimum in temperature is produced. This develops towards a profile form with two distinct peaks, not dissimilar to the work of Bosse and Griewank (2014) as the discretisation level increases beyond 18. These differences indicate that the discretisation level can have significant bearing on the specific profile being produced with this method, however in most cases the overall solution form does not differ as drastically. It is shown that as N is increased the attainable value for the objective function (Eq. 13) increases, as expected due to the greater level of control possible with a higher number of manipulatible sections in the temperature profile.

3.2.2.2 Effect of initialising temperature profile.

An immediate observation is that solutions do not converge to the same profile, meaning that globally optimal solutions are not being produced, rather the input initialising profile has significant impact on the profile output for any set of conditions when using this methodology. However, there exists a large number of similarities between many of the solution profiles' appearance, with significant features present across all solutions even when differences in the duration or magnitude of these features exists. It is found that cases A-C all tend towards the same solution form with a single peak.

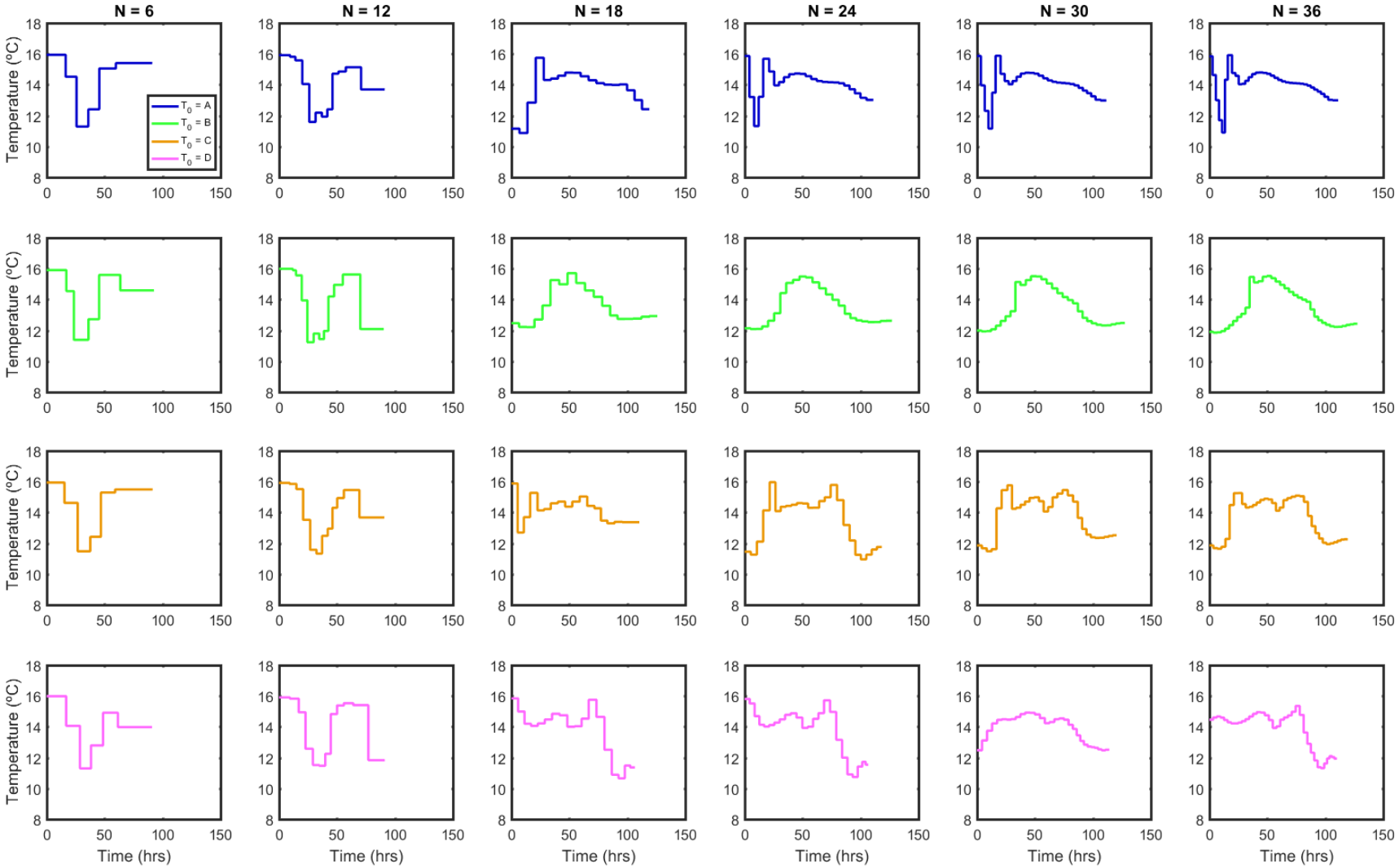

Figure 16. T(t) solutions from CP with fmincon and finite difference derivatives, for various initialisations (T_0) and discretisation levels (N), $W_t = 0.5$, $W_E = 0.5$.

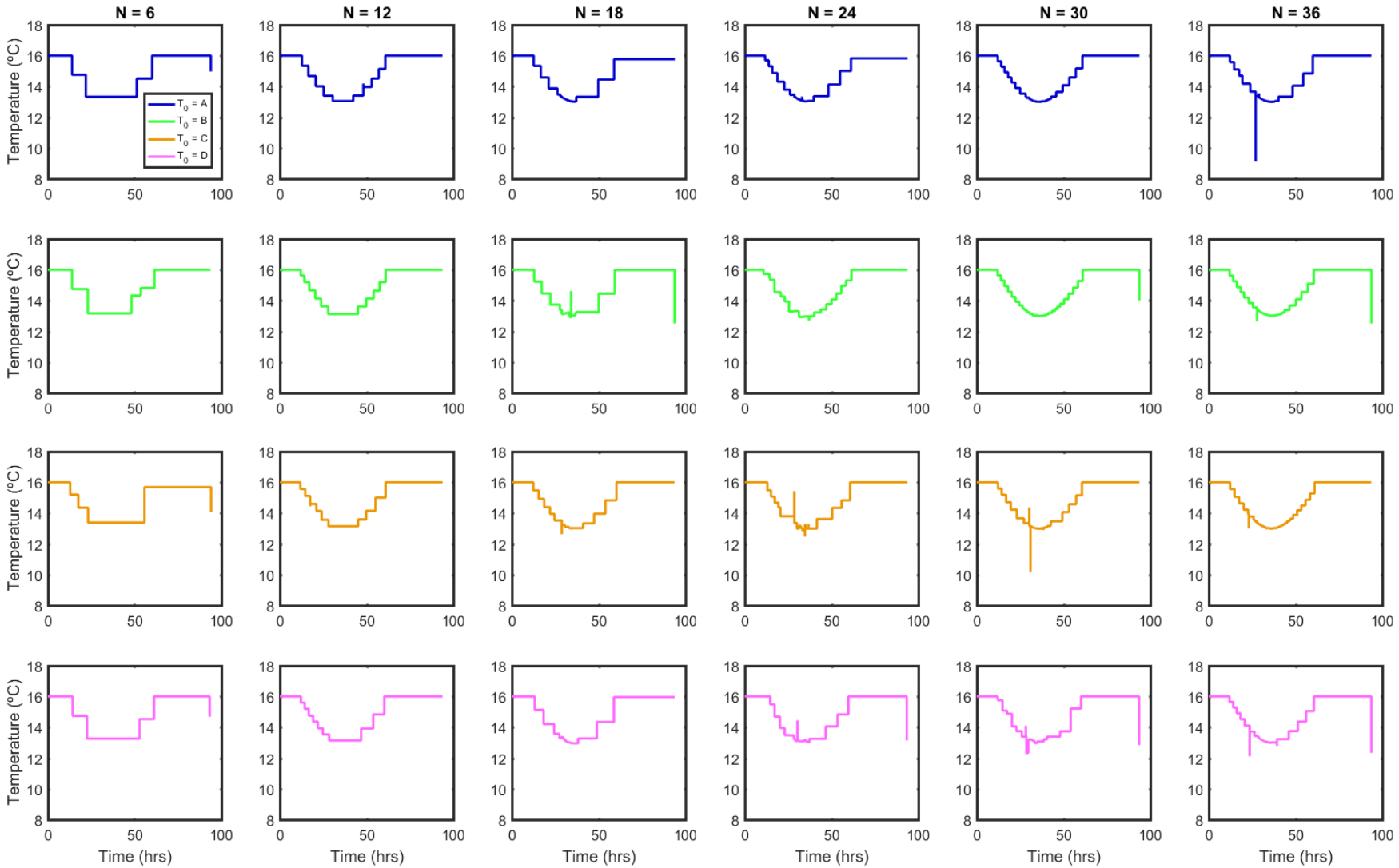

Figure 17. T(t) solutions from CP with IPOPT and analytical first derivatives, for various initialisations (T_0) and discretisation levels (N), $W_t = 0.25$, $W_E = 0.75$.

3.2.2.3 Control Profile Performance

The upper row in Fig. 18 compares the performance of the profiles computed for N = 42 with each initialising isothermal profile considered.

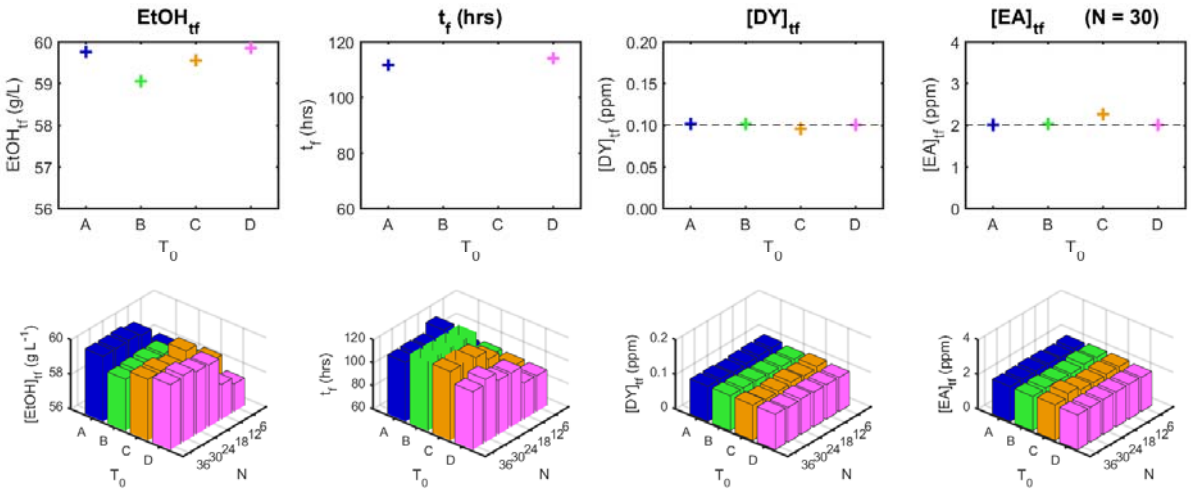

Figure 18. Influence of discretisation level (N) and initialising isothermal profile (T_0) on piecewise linear profile performance - CP with fmincon, novel initialisation profiles.

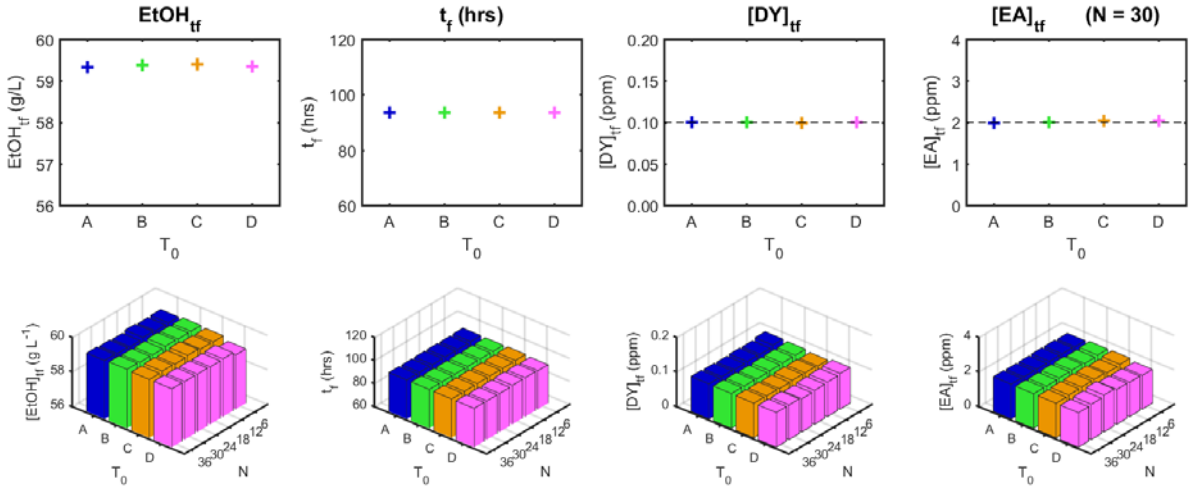

Figure 19. Influence of discretisation level (N) and initialising isothermal profile (T_0) on piecewise linear profile performance - CP with IPOPT, novel initialisation profiles.

Firstly, the left most plot shows the product ethanol concentration: all profiles are producing high concentration (59-60 g L^{-1}). The next plot similarly shows batch times: while all cases represent acceptable batch durations, significant variation exists between the values for the four cases considered, ranging from 110 to 130 hours. The last two plots in top row depict the by-product concentration levels, highlighting that for this discretisation level (N = 42) all profiles satisfy the constraint thresholds. The second row of plots in Fig. 18 considers a third axis to visualise the

effect of discretisation level on the resulting fermentation performance. The general trend observed is that as the discretisation level increases the attainable ethanol concentration also increases.

Conversely the batch time actually increases with N, however at a lesser relative rate such that the objective still improves with N. An interesting exception to this trend is profile B which shows very little variation of batch time with discretisation level. The last two 3D bar graphs show by-product levels for all solution profiles. It is seen that there is one anomaly: a single profile where the ethyl acetate constraint (Eq. 14), is not satisfied. It can be seen that there are other cases where very slight violations exist, however these can be attributed to the slight deviations that exist between the performance of the profile during the NLP algorithm and later integration of the solution, depending on the accuracy of the piecewise polynomial representation of the continuous state trajectories in the NLP formulation. Deviations are shown to be non-significant as the algorithm used captures the state trajectories effectively.

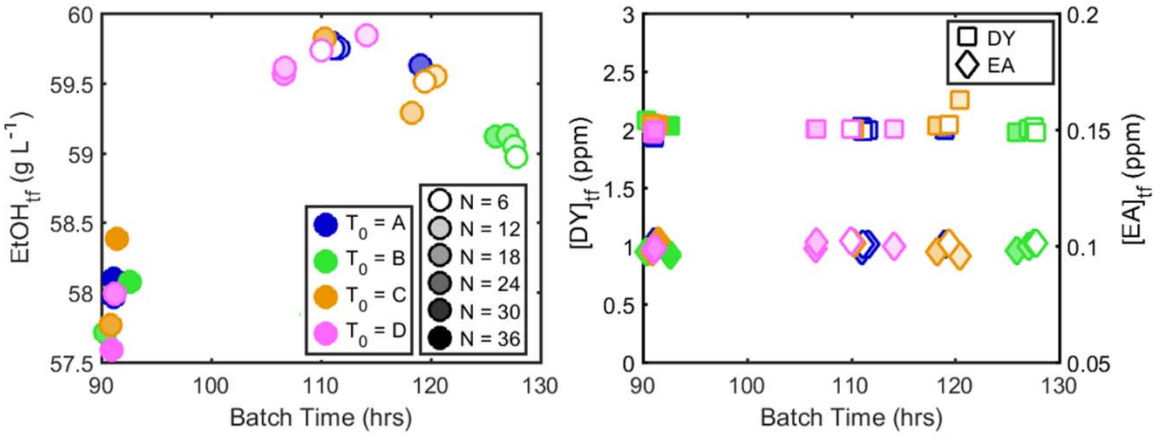

Figure 20. Effect of initialising profile (T_0), and discretisation (N) on fermentation performance: fmincon.

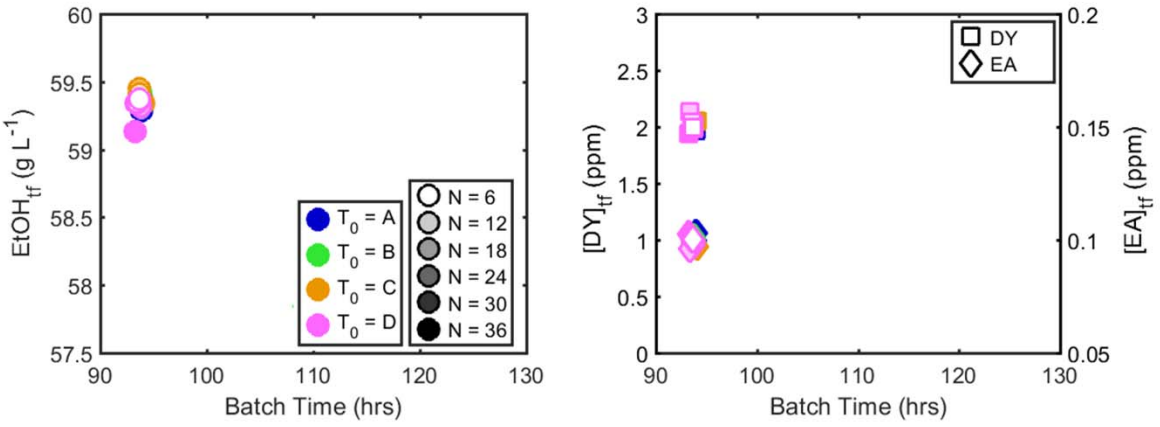

Figure 21. Effect of initialising profile (T_0), and discretisation (N) on fermentation performance: IPOPT.

Figures 20-21 show an alternative performance plot of the output profiles computed. Plotting batch time against ethanol concentration represents the bi-criteria objective function, where the most favourable solutions would exist in the upper left corner. The second in plot Fig. 20 represents the by-product levels as a function of discretisation level for each initialising solution. Near universal constraint satisfaction is again shown: while many markers lie marginally (< 10%) above the threshold level, this is again attributed to the accuracy of the piecewise approximation of the state trajectories, and is not detrimental to the applicability and usefulness of the resultant profiles produced.

4. Conclusions

A control vector parameterisation strategy has been used to compute temperature profiles to minimise a bi-criteria problem considering ethanol maximisation and batch time minimisation. An interior point NLP algorithm (IPOPT) has been used to determine both piecewise constant (stepwise) and piecewise linear temperature profiles, for a range of levels of discretisation and initialising temperature profiles. It is found that higher degrees of discretisation permit an improved objective due to the greater degrees of path freedom. Similarly, it is shown that piecewise linear profiles have greater attainable performance for the same reason, with the additional benefit that the removal of instantaneous temperature gradients leads to the piecewise linear profiles being industrially implementable. It has been found that in several high discretisation cases it has not been possible to satisfy the imposed constraint on diacetyl, limiting the usefulness of the results obtained with this methodology.

An additional sequential dynamic optimisation procedure has been performed using the Dynopt package for MATLAB. Discretising the state trajectories in addition to the control vector using orthogonal collocations permits a large scale NLP problem to be solved, here for piecewise constant temperature profiles. Similarly, a range of N, T_0 cases have been solved: it is found that the lowest discretisation levels produce control profiles with the most favourable objective. This counter-intuitive result is indicative of the limitations of the simultaneous dynamic optimisation methodology employed, however it does not discredit the substantial process improvements the produced profiles are capable of. It has been demonstrated that the Dynopt package is capable of computing temperature profiles for efficient fermentation, which universally fulfil the imposed by-product constraints. The solution produced is still sensitive to the input profile used to initiate the solver, which if drastically different from the preferred path can produce sporadic, undesirable profiles. It is demonstrated that the attainable performance of the resultant output profile has a strong dependence on discretisation level, with the solution form differing when there is a lesser number of control profile segments. Once the discretisation level is suffice to describe the preferred path adequately, further increments are found to be less significant.

Interestingly, comparing the manipulation profiles computed by the two differing methodologies shows significantly differing profile forms. The differences are drastic: the sequential profiles show a very drastic temperature reduction around the active cell concentration maxima, meanwhile the results obtained from Dynopt (sequential) favour a far less significant temperature reduction during this stage. It is remarkable that, excluding the numerous cases of constraint violation, the performance of the profiles produced by the two methods have performance which is not drastically different, despite the significant differences in their form.

It is demonstrated that blind initial guesses severely restrict the performance of output profiles from the dynamic optimisation methodologies. Electing to initialise with promising candidate profiles is shown to be highly beneficial, with the simultaneous optimisation approach being able to improve upon the input profiles in all cases. It is however shown that the input profile does restrict the solution form, so a range of cases should be considered to allow an extensive search for the most preferable output profiles to be performed. The robustness and computational performance of the interior point NLP solver (IPOPT) is clearly superior to that of the alternative solver (Dynopt) considered: while global optimisation is not the purpose of the present study, it is clear that poor initialisations result in suboptimal temperature manipulation profiles, but also that the form of the solutions obtained (e.g. high initial temperature, progressive cooling and reheating) carry technical merit with respect to plant implementations (e.g. feeding warm wort to the fermentor straight from the mashing stage under insulation, rather than allowing cooling).

Acknowledgements

The authors gratefully acknowledge the financial support of the Eric Birse Charitable Trust for a Birse Doctoral Fellowship awarded to Mr. A.D. Rodman, and that of the Engineering and Physical Sciences Research Council (EPSRC) via funding from an Impact Acceleration Account (IAA) administered by Edinburgh Research & Innovation (ERI). Moreover, they express their thanks to Mrs Hilary Jones, Mr Simon P. Roberts and Mr Udo Zimmermann (WEST Beer) and Mr Roddy McEwan (Molson Coors) for encouragement and inspiring discussions throughout this project. Dr. Dimitrios I. Gerogiorgis gratefully acknowledges a Royal Academy of Engineering (RAEng) Industrial Fellowship.

Nomenclature

Roman symbols

C	Concentration (g/L, ppm)
DY	Diacetyl (-)
EtOH	Ethanol (-)
EA	Ethyl Acetate (-)
J_{MIN}	Objective value (-)
S	Sugar (-)
T	Fermenter temperature (°C)
W_t	Objective time weight (%)
W_E	Objective ethanol weight (%)
X_A	Active biomass concentration (g L^{-1})
X_D	Dead biomass concentration (g L^{-1})
X_L	Latent biomass concentration (g L^{-1})
Y_{EA}	Ethyl acetate production stoichiometric factor (g L^{-1})
f	Fermentation inhibition factor (g L^{-1})
k_e	Ethanol affinity constant (g L^{-1})
k_s	Sugar affinity constant (g L^{-1})
k_x	Biomass affinity constant (g L^{-1})
t	Time (h)
t_f	Batch time (h)
J	Jacobian (-)
H	Hessian (-)
s	Slack variables (-)
S	Diagonal of s (-)
g	Inequality constraint function (-)
h	Equality constraint function (-)
u	Decision vector (-)
y	Lagrange multiplier vector (-)
e	Vector of ones (-)
N	Discretisation level (-)
T_0	Initialising solution (-)
x_{K_x}	Piecewise state trajectory approximation (-)
x_{K_u}	Piecewise control trajectory approximation (-)

Greek symbols

λ	Lagrange multiplier
Λ	Diagonal of λ
μ	Barrier parameter
μ_{AB}	Diacetyl consumption rate (g^{-1} h^{-1} L)
μ_{DT}	Specific cell death rate (h^{-1})
μ_{DY}	Diacetyl production rate (g^{-1} h^{-1} L)
μ_E	Ethanol production rate (h^{-1})
μ_L	Specific cell activation rate (h^{-1})
μ_S	Sugar consumption rate (h^{-1})
μ_{SD}	Specific dead cell settling rate (h^{-1})
μ_x	Specific cell growth rate (h^{-1})
ϕ_j	Basis function (-)
θ_j	Basis function (-)

Subscripts and operators

$\widetilde{(\ )}$	Normalised parameter (-)
$(\ )_0$	Initial condition (-)

References

1. Almeida Nt, E., and Secchi, A. R., 2011. Dynamic optimization of a FCC converter unit: numerical analysis. *Brazilian Journal of Chemical Engineering*, **28**(1): 117-136.
2. Arpornwichanop, A., Kittisupakorn, A., Mujtaba, I.M., 2005. On-line dynamic optimization and control strategy for improving the performance of batch reactors, *Chemical Engineering & Processing*, **44**(1): 101-114.
3. Aziz, N. and Mujtaba, I.M., 2002. Optimal operation policies in batch reactors. *Chemical Engineering Journal*, **85**(2-3): 313-325.
4. Biegler, L. T., 2010. Nonlinear programming: concepts, algorithms, and applications to chemical processes. SIAM publishing. Print.
5. Biegler, L. T., Campbell, S. L. and Mehrmann, V., 2012. Control and optimization with differential-algebraic constraints. SIAM publishing. Print.
6. Biegler, L. T., Cervantes, A. M. and Wächter, A., 2002. Advances in simultaneous strategies for dynamic process optimization. *Optimization, Chemical Engineering Science*, **57**: 575-593.
7. Bosse, T. and Griewank, A., 2014. Optimal control of beer fermentation processes with Lipschitz-constraint on the control. *Journal of the Institute of Brewing*, **120**(4): 444-458.
8. Byrd, R. H., Gilbert, J. C. and Nocedal, J., 2000. A Trust Region Method Based on Interior Point Techniques for Nonlinear Programming. *Mathematical Programming*, **89**(1): 149–185.
9. Carrillo-Ureta, G., Roberts, P. and Becerra, V., 2001. Genetic algorithms for optimal control of beer fermentation. *Proceedings of the IEEE International Symposium on Intelligent Control*, 391-396.
10. Cervantes, A. and Biegler, L. T., 1998. Large-scale DAE optimization using a simultaneous NLP formulation. *AIChE Journal*, **44**(5): 1038-1050.
11. Cervantes, A., Wachter, A., Tutuncu, R. H. and Biegler, L. T., 2000. A reduced space interior point strategy for optimization of differential algebraic systems. *Computers and Chemical Engineering*, **24**: 39-51.
12. Cizniar, M., Fikar M, and Latifi, M.A., 2006. MATLAB Dynamic Optimisation Code DYNOPT, User's guide, Technical Report, KIRP FCHPT STU, Bratislava.
13. Currie, J. and Wilson D. I., 2017. OPTI: Lowering the Barrier Between Open Source Optimizers and the Industrial MATLAB User, *Foundations of Computer-Aided Process Operations,* Georgia, USA.
14. de Andrés-Toro, B., Giron-Sierra, J., Lopez-Orozco, J. and Fernandez-Conde, C., 1997. Using genetic algorithms for dynamic optimization: an industrial fermentation case. *Proceedings of the 36th IEEE Conference on Decision and Control*, **1**: 828-829.
15. de Andrés-Toro, B., Giron-Sierra, J., Lopez-Orozco, J., and Fernandez-Conde, C., 1998. A kinetic model for beer production under industrial operational conditions. *Mathematics and Computers in Simulation*, **48**(1): 65-74.
16. Denbigh, K.G., 1958. Optimum temperature sequences in reactors. *Chemical Engineering Science*, **8**(1-2): 125-132.
17. Dormand, J. R. and P. J. Prince, 1980. A family of embedded Runge-Kutta formulae, *J. Comp. Appl. Math*., **6**: 19–26.
18. Ferrari, A., Gutierrez, S., Biscaia, E.C., Jr., 2010. Development of an optimal operation strategy in a sequential batch reactor (SBR) through mixed-integer particle swarm dynamic optimization (PSO), *Computers & Chemical Engineering* , **34**(12): 1994-1998.
19. Gee, D. A. and Ramirez, W. F., 1988. Optimal temperature control for batch beer fermentation. *Biotechnology and Bioengineering*, **31**: 224-234.
20. Hanke, S., Ditz, V., Herrmann, M., Back, W., Becker, T and Krottenthaler, M., 2010. Influence of ethyl acetate, isoamyl acetate and linalool on off-flavour perception in beer. *Brewing Science*, **63**(7): 94-99.
21. Izquierdo-Ferrero, J. M., Fernández-Romero, J. M., Luque de Castro, M. D., 1997. On-line flow injection–pervaporation of beer samples for the determination of diacetyl. *The Analyst*, **122**(2): 119-122.
22. Logsdon, J.S. and Biegler, L.T., 1993. A relaxed reduced space SQP strategy for dynamic optimization problems, *Computers & Chemical Engineering* **17**(4): 367-372.
23. Logsdon, J.S., 1990. Efficient determination of optimal control profiles for differential algebraic systems, PhD Thesis, Carnegie Mellon University.
24. Luus, R., 1994. Optimal control of batch reactors by iterative dynamic programming. *Journal of Process Control*, **4**(4): 218-226.

25. Mohan, S.V., Rao, N.C., Prasad, K.K., Krishna, P.M., Rao, R.S., Sarma, P.N., 2005. Anaerobic treatment of complex chemical wastewater in a sequencing batch biofilm reactor: Process optimization and evaluation of factor interactions using the Taguchi dynamic DOE methodology, *Biotechnology & Bioengineering*, **90**(6): 732-745.
26. Mujtaba, I. M. and Macchietto, S., 1993. Optimal operation of multicomponent batch distillation-multiperiod formulation and solution. *Computers and Chemical Engineering*. **17**(12): 1191-1207.
27. Nocedal, J., Wächter, A. and Waltz, R.A., 2009. Adaptive barrier update strategies for nonlinear interior methods. *SIAM Journal on Optimization*, **19**(4):1674-1693.
28. Osorio, D., Pérez-Correa, J. R., Biegler, L. T. and Agosin, E., 2005. Wine distillates: practical operating recipe formulation for stills. *Journal of Agricultural and Food Chemistry*, **53**(16): 6326-6331.
29. Patel, N., Padhiyar, N., 2017. Multi-objective dynamic optimization study of fed-batch bio-reactor, *Chemical Engineering Research & Design*, **119**: 160-170.
30. Rodman, A. D. and Gerogiorgis. D. I., 2016a. Multi-objective process optimisation of beer fermentation via dynamic simulation. *Food and Bioproducts Processing*, **100**: 255-274.
31. Rodman, A. D. and Gerogiorgis. D. I., 2016b. Dynamic simulation and visualisation of fermentation: Effect of process conditions on beer quality. *IFAC-PapersOnLine,* **49**(7): 615-620.
32. Shampine, L. F. and M. W. Reichelt, 1997. The MATLAB ODE Suite, *SIAM Journal on Scientific Computing*, **18**: 1–22.
33. Sørensen, E., Macchietto, S., Stuart, G. and Skogestad, S., 1996. Optimal control and on-line operation of reactive batch distillation. *Computers and Chemical Engineering*, **20**(12): 1491-1498.
34. Trelea, I. C., Titica, M., Landaud, S., Latrille, E., Corrieu, G. and Cheruy, A., 2001. Predictive modelling of brewing fermentation: from knowledge-based to black-box models. *Mathematics and Computers in Simulation*, **56**(4): 405-424.
35. Vanderhaegen, B., Neven, H., Verachtert, H. and Derdelinckx, G., 2006. The chemistry of beer aging – a critical review. *Food Chemistry*, **95**(3): 357-381.
36. Wächter, A. and Biegler, L.T., 2005a. Line search filter methods for nonlinear programming: Motivation and global convergence. *SIAM Journal on Optimization*, **16**(1): 1-31.
37. Wächter, A. and Biegler, L.T., 2005b. Line search filter methods for nonlinear programming: Local convergence. *SIAM Journal on Optimization*, **16**(1): 32-48.
38. Wächter, A., 2002. An interior point algorithm for large-scale nonlinear optimization with applications in process engineering. *PhD Thesis*, Carnegie Mellon University, Pittsburgh, PA, USA.
39. Wajge, R.M., Gupta, S.K., 1994. Multiobjective dynamic optimization of a nonvaporizing Nylon-6 batch reactor, *Polymer Engineering and Science* **34**(15): 1161-1172.
40. Waltz, R. A., Morales, J. L., Nocedal, J. and Orban, D., 2006. An interior algorithm for nonlinear optimization that combines line search and trust region steps, *Mathematical Programming*, **107**(3): 391–408.
41. Xiao, J., Zhou, Z., Zhang, G., 2003. Ant colony system algorithm for the optimization of beer fermentation control. *Journal of Zhejiang University SCIENCE*, **5**(12): 1597-1603.
42. Zapata, R.B., Villa, A.L., de Correa, C.M., Ricardez-Sandoval, L., Elkamel, A., 2010. Dynamic modeling and optimization of a batch reactor for limonene epoxidation, *Industrial & Engineering Chemistry Research*, **49**(18): 8369-8378.
43. Zavala, V.M., Flores-Tlacuahuac, A., Vivaldo-Lima, E., 2005. Dynamic optimization of a semi-batch reactor for polyurethane production, *Chemical Engineering Science* **60**(11): 3061-3079.